NASA CONTRACTOR REPORT

NASA CR-2050

A DIRECT NUMERICAL METHOD FOR PREDICTING CONCENTRATION PROFILES IN A TURBULENT BOUNDARY LAYER OVER A FLAT PLATE

by James W. Dow

Prepared by
MISSISSIPPI STATE UNIVERSITY
State College, Miss.
for George C. Marshall Space Flight Center

NATIONAL AERONAUTICS AND SPACE ADMINISTRATION • WASHINGTON, D. C. • JUNE 1972

TECHNICAL REPORT STANDARD TITLE PAGE

1. REPORT NO.	2. GOVERNMENT ACCESSION NO.	3. RECIPIENT'S CATALOG NO.
NASA CR-2050		

4. TITLE AND SUBTITLE	5. REPORT DATE
A DIRECT NUMERICAL METHOD FOR PREDICTING CONCENTRATION PROFILES IN A TURBULENT BOUNDARY LAYER OVER A FLAT PLATE	June 1972
	6. PERFORMING ORGANIZATION CODE

7. AUTHOR(S)	8. PERFORMING ORGANIZATION REPORT #
James W. Dow	IES-72-02-001

9. PERFORMING ORGANIZATION NAME AND ADDRESS	10. WORK UNIT NO.
Institute for Environmental Studies Mississippi State University State College, Mississippi	11. CONTRACT OR GRANT NO. NGL 25-001-32
	13. TYPE OF REPORT & PERIOD COVERED
12. SPONSORING AGENCY NAME AND ADDRESS	CONTRACTOR REPORT
NASA Washington, D. C. 20546	14. SPONSORING AGENCY CODE

15. SUPPLEMENTARY NOTES

16. ABSTRACT

A numerical solution of the turbulent mass transport equation utilizing the concept of eddy diffusivity is presented as an efficient method of investigating turbulent mass trasnport in boundary layer type flows. A Fortran computer program is used to study the two-dimensional diffusion of ammonia, from a line source on the surface, into a turbulent boundary layer over a flat plate. The results of the numerical solution are compared with experimental data to verify the results of the solution. Several other solutions to diffusion problems are presented to illustrate the versatility of the computer program and to provide some insight into the problem of mass diffusion as a whole.

17. KEY WORDS	18. DISTRIBUTION STATEMENT
Diffusion, Eddy diffusivity, Turbulent mass transport, flat plate	

19. SECURITY CLASSIF. (of this report)	20. SECURITY CLASSIF. (of this page)	21. NO. OF PAGES	22. PRICE
Unclassified	Unclassified	105	$3.00

*For sale by the National Technical Information Service, Springfield, Virginia 22151

ACKNOWLEDGMENTS

The author wishes to express sincere appreciation to Dr. Richard Forbes of the Mechanical Engineering Department, my supervising professor, for his invaluable guidance and assistance. Also, I wish to thank Dr. W. Steve Shepard, Dr. Joe F. Thompson, and Dr. Z. U. A. Warsi of the Aerophysics and Aerospace Engineering Department for their assistance which directly contributed to the successful completion of this study.

The financial support provided by NASA Grant NGL 25-001-032 is greatly appreciated.

J.W.D.

State College, Mississippi

January, 1972

A Thesis
Submitted to the Faculty of
Mississippi State University
in Partial Fulfillment of the Requirements
for the Degree of Master of Science
in the Department of
Aerophysics and Aerospace Engineering

State College, Mississippi

January, 1972

TABLE OF CONTENTS

TABLE OF CONTENTS (Continued)

LIST OF SYMBOLS

A	constant in numerical solution, local, constant in logarithmic velocity profile approximation
a	constant in power law velocity profile approximation
B	constant in numerical solution, local, constant in logarithmic velocity profile approximation
b	constant in power law velocity profile approximation
C	constant in numerical solution, local
c	local concentration
c_o	maximum concentration at source
D	constant in numerical solution, local
G	mass flux in experimental data, mg./cm.·s
I	number of Δx-steps in two dimensional field
i	x-index in finite difference formulation
J	number of Δy-steps in two-dimensional field
j	y-index in finite difference formulation
K	function defined for stability analysis
k(y)	arbitrary function in distribution of eddy diffusivity coefficient
L_x	length of field in x-direction, ft.
L_y	length of field in y-direction, ft.
L_δ	rate of change of growth of boundary layer thickness
L_λ	rate of change of growth of plume
NSIY	number of Δy-steps inside the boundary layer at trailing edge of field
n	time index in finite difference formulation
Q	constant in power formula approximation for ψ
q	mass flux

R	the local partial derivative of ψ with respect to y
t	time
U_∞	freestream velocity, ft/s
u	local x-component of velocity
u_*	shear velocity
V_s	mean fall velocity of contaminant
$\underline{v}$	local y-component of fluid velocity
v	$\underline{v} + V_s$, composite vertical velocity
X	distance downstream of leading edge of the flat plate ft.
x	distance downstream of source, cm.
y	vertical distance above flat plate

Physical Increments

Δt	time step size
Δx	step size in x-direction
Δy	step size in y-direction

Greek Symbols

α	y/λ
β	measure of relative rates of growth of plume and boundary layer thickness
ξ	molecular plus turbulent momentum diffusivity coefficient
$\overline{\xi}$	depth averaged momentum diffusivity coefficient
δ	boundary layer thickness
ε	constant for convergence criteria
ε_m	momentum eddy diffusivity coefficient

ε_y mass eddy diffusivity coefficient

η nondimensional height based on the vertical distance, y

$\eta_\delta = \frac{u*\delta}{\nu}$, nondimensional height based on the boundary layer thickness,

λ characteristic plume height

ν kinematic viscosity, f^2/s

ρ fluid density, $slug/ft^3$

τ local shearing stress

τ_w wall shearing stress

ϕ nondimensional velocity in logarithmic velocity profile approximation

χ molecular mass diffusion coefficient

χ_1 molecular plus turbulent mass diffusion coefficient

ψ nondimensional transfer coefficient

Special Symbols

$\overline{u'c'}$ time averaged turbulent concentration fluctuation

$\overline{u'v'}$ time averaged turbulent velocity fluctuation

x/δ_{AV} nondimensional distance from source

' the primed notation implies a non-dimensional quantity

$\bar{}$ barred terms are time averages of turbulent quantities or depth averaged terms

Subscripts

m designation for momentum eddy diffusivity coefficient

s designation for source location, also mean fall velocity

T	designation for total distance from leading edge of plate to trailing edge of concentration field
w	wall or surface conditions
x	along x-coordinate
y	along y-coordinate, also designates mass eddy diffusivity coefficient
δ	associated with local boundary layer thickness
∞	designates free stream conditions
*	designates footnote for reference, or shear velocity

LIST OF ILLUSTRATIONS AND TABLES

FIGURE Page

TABLE Page

I. INTRODUCTION

The exact nature of transport and mixing processes in turbulent flows has long intrigued designers and engineers. More recently, the problems encountered in waste dispersion have stimulated interest in the area of turbulent diffusion. Since the source of most industrial and chemical contaminants is in many cases close to solid boundaries, the study of mass diffusion in a turbulent boundary layer is of special interest.

In this investigation the characteristics of the propagation of an impurity injected into the boundary layer over a flat plate with zero longitudinal pressure gradient will be studied on the basis of a numerical solution of the turbulent diffusion equation. In order to determine the validity of the numerical solution, the predicted results are compared to experimental data for a practical diffusion problem; and finally, several solutions are presented to provide some additional insight into the mechanics of the turbulent diffusion process.

II. RELATED INVESTIGATIONS

In 1921 G. I. Taylor [15]* discussed diffusion of material through the interior of a fluid using a statistical approach. He attempted to show that the statistical properties of a fluid flow were sufficient to determine the law which governs the average distribution of particles initially concentrated at one point, at any subsequent time.

In 1931 O. G. Sutton [16] extended the work of Taylor to define an "effective" eddy diffusivity and diffusion coefficient which would remain constant "over a field of a few hundred meters to hundreds of kilometers." His approach was also entirely statistical, and no attempt was made to solve the problem with respect to the physical properties of the fluid.

By 1950, the importance of the physical properties of the ambient fluid, with respect to the diffusion process, were being investigated; and the concept of eddy transport was being utilized. In 1954 A. S. Monin and A. M. Obukhov [17] investigated the process of "turbulent mixing in the ground layer of the atmosphere on the basis of the theory of similitude," and the numerical parameters involved in

---

*The number in brackets refers to a reference source listed in the bibliography.

atmospheric diffusion were more exactly determined using empirical data from wind gradient observations made in the USSR. Working formulas were obtained from this study for determining the basic diffusion characteristics of the ground layer, the layer of air immediately above the earth's surface.

In 1962 Poreh and Cermak [9] summarized some experimental work involving the diffusion of mass from a surface-level line source into a boundary layer over a flat plate. From the experimental data they formulated relations based on a concept of eddy diffusivity to describe the mechanics of the diffusion process.

In 1963, Morkovin [3] extended the work of Poreh and Cermak to consider the correlation between the results of the experimental work [9], the concepts of eddy diffusivity, and the turbulent Schmidt number (the ratio of momentum diffusion to mass diffusion) and the Prandtl number (the ratio of momentum diffusion to heat diffusion). Morkovin concluded that (a) the shape of the quasi-similar concentration profiles of Poreh and Cermak were consistent with the concept of eddy diffusivity; (b) when the velocity profiles of the boundary layer were locally simulated by power profiles, the concept of eddy diffusivity led to the experimentally observed result that in the first approximation the pollutant plume grew independently of the free-stream velocity U_∞; (c) the concentration profile characteristics were governed essentially by an eddy diffusivity

in the core of the turbulent layer and a smooth intermittency cut-off as the edge of the layer was reached; and (d) "The diffusivity coefficients depend upon the local characteristic scales of the diffusing fields, which change during the course of their development even in the presence of more or less invariant eddy structure of the surrounding field." Thus the so-called turbulent Schmidt number is not an absolute number, but it depends upon the relative development of the turbulent velocity field and the scalar diffusing field. Morkovin divided the boundary layer into five analytical segments to account for variations in the coefficient of eddy diffusivity: (a) a laminar sublayer, (b) a buffer layer, (c) a "logarithmic" regime, (d) an inertially controlled layer, and (e) a layer extending into the freestream to approximate the intermittency drop-off. The precise definition of the limits or boundaries of these layers could present certain difficulties when modeling various flow problems.

In 1969, Sayre [2] investigated the dispersion of silt in an open channel using a technique which considered a continuous variation of the eddy diffusivity coefficient in the vertical direction. In his work, Sayre considered only the turbulent transport of mass and expressed his results in terms of a moment transformation for the diffused mass distribution along the axis of the flow. Although this method was accomplished with no loss of rigor, some of the detail was lost. This work involved the introduction of a

concentration profile into a volume and then following the volume downstream as the diffusion process progressed.

In 1970, Jobson and Sayer [1] extended the work of Sayer [2] to include a numerical approximation to the steady state solution of the turbulent diffusion equation to predict concentration profiles in open channels. This approach used an eddy diffusivity which varied as a function of the vertical distance from the lower boundary of the channel. Again only turbulent transfer was considered. Their results agreed well with experimental data.

In the following pages, specific segments of information are taken from designated references to develop the theory utilized in this investigation.

III. DISCUSSION OF THE PROBLEM

In general, the problem of diffusion is to express the turbulent transport of some scalar quantity in terms of statistical functions of the turbulent motion and of the boundary conditions. A complete solution of the transport problem can be obtained only if there is a complete knowledge of the turbulent motion. To overcome the difficulties involved in completely describing the complex turbulent motion, the concept of "eddy diffusivity" has been used in meteorological and engineering studies.

Theories utilizing this concept have attempted to relate the mean flux of the contaminant by turbulent fluctuations to known variables of the turbulent field at the same point. The assumption that this flux $q_i = \overline{u_i' c'}$ is proportional to the gradient of the concentration $(\partial c/\partial x_i)$ provides that the flux normal to the stream become $q_y = v'c' = - \varepsilon_y(\partial c/\partial y)$ where ε_y represents the mass coefficient of eddy diffusivity. This mass coefficient of eddy diffusivity is analogous to the coefficient of molecular diffusivity. The mass coefficient of eddy diffusivity has been introduced as a mathematical operation in an attempt to simplify the problem. Such a process has been found successful in studies of free turbulence [8] where ε_y may be approximated by a constant.

In a boundary layer ε_y is not equal to a constant [9], and success has been reported in relating ε_y to turbulent quantities such as $-[(\overline{u'v'})/(\partial u/\partial y)]$ which corresponds to an eddy diffusivity for momentum transfer. This latter model was reported to have been productive in a few cases of diffusion, in homogeneous turbulence, from an area source where a continuous flux of matter was emitted from a boundary [11]. Such models usually divide the flow into distinct layers and zones with an approximate value of ε_y assigned to each layer and zone.

In this investigation a relation between the coefficient of eddy diffusivity for mass and momentum transport is obtained which is continuous through the boundary layer and is applicable for relatively large longitudinal distances along the direction of the flow in the boundary layer. Also, this relation accounts for the molecular diffusion processes in both the so-called laminar sublayer and the freestream above the boundary layer.

Utilization of the concept of eddy diffusivity and the application of the principle of conservation of mass to an incremental volume of flow yields the basic mass transfer equation. This equation, see Sayre [18], is

$$\frac{\partial \bar{c}_i}{\partial t} + \bar{u}_j \frac{\partial \bar{c}_i}{\partial x_j} = \frac{\partial}{\partial x_j}\left[\varkappa \frac{\partial \bar{c}_i}{\partial x_j} - \overline{c_i' u_j'} \right] \tag{1}$$

which may be written as

$$\frac{\partial \bar{c}_i}{\partial t} + \bar{u}_j \frac{\partial \bar{c}_i}{\partial x_j} = \frac{\partial}{\partial x_j}\left[\chi_1 \frac{\partial \bar{c}_i}{\partial x_j} \right] \qquad (2)$$

where $\chi_1 = \chi + \epsilon_y$.

In equation (2), c represents the concentration of the transferable scalar quantity: t = time; u_j = the local convective velocity in the j^{th} direction; x_j = the j^{th} coordinate direction; and χ = the molecular diffusivity coefficient.

The coordinate system used in this investigation is shown in Figure 1, with x representing the direction of the freestream, the y-axis is oriented along the vertical, and the z-axis lies in the horizontal plane normal to the x-y plane.

The expansion of equation (2) yields (Drop Bar Notation)

$$\frac{\partial c}{\partial t} + u\frac{\partial c}{\partial x} = \frac{\partial}{\partial y}\left[\chi_1 \frac{\partial c}{\partial y} - vc \right] + \epsilon_x \frac{\partial^2 c}{\partial x^2} + c\frac{\partial v}{\partial y} \qquad (3)$$

where ϵ_x represents the x-component of the eddy diffusivity coefficient for mass transport. Jobson [1] has shown that the longitudinal gradients are on the order of one percent (1%) of the vertical gradients. Therefore the longitudinal diffusion term $\epsilon_x(\partial^2 c/\partial x^2)$ is neglected in this analysis, and equation (3) becomes

$$\frac{\partial c}{\partial t} + u\frac{\partial c}{\partial x} = \frac{\partial}{\partial y}\left[\chi_1 \frac{\partial c}{\partial y} - vc \right] + c\frac{\partial v}{\partial y} \qquad (4)$$

Equation (4) represents the governing equation for turbulent mass transport in a two dimensional boundary layer type flow.

In addition to the simplification previously introduced, it is further assumed that the contaminant is introduced into the flow in a quantity and with a velocity such that the local flow velocities are negligibly affected. The density of the contaminant is assumed to be approximately that of the ambient fluid. Hence the contaminant is neutrally bouyant. These assumptions uncouple the solution of the diffusion equation from any solution of the velocity field over the flat plate.

For the turbulent flows of interest, the velocity field is usually approximated by some form of either a logarithmic or a power law profile. For comparison purposes, two different forms of approximations were used to describe the velocity field in the two dimensional turbulent boundary layer over the flat plate. The first approximation was the universal logarithmic profile

$$\phi = A \ln \eta + B \tag{5}$$

where $\phi = \frac{u}{u_*}$ $\eta = \frac{y u_*}{\nu}$ and $u_* = \sqrt{\frac{\tau_w}{\rho}}$ = shear velocity [8]. Equation (5) is valid for $5 \leq \eta \leq \eta_\delta$ and for Reynolds numbers less than 10^6. For $\eta < 5$, a linear profile is assumed, $\frac{u}{u_*} = \eta$.

The second approximation represents the power-law form as

$$\frac{u}{U_\infty} = a\left(\frac{y}{\delta}\right)^b \tag{6}$$

where δ = the boundary layer thickness, a = 1.0, and b = 1/7 for this investigation [8].

Equations (5) and (6) were used to provide the x-component of velocity throughout the field. Once this was accomplished, the continuity equation was integrated using the trapezoidal rule to obtain the vertical component of the local velocity. The error introduced by this method was of the order $(\Delta y)^3$ at every step [8].

For a complete analysis for the determination of the velocity field, see Appendix A. With the velocity field established, the problem remains to solve for the point concentration throughout the field.

IV. NUMERICAL SOLUTION OF THE TURBULENT DIFFUSION EQUATION

The turbulent diffusion equation is written as

$$\frac{\partial c}{\partial t} + u \frac{\partial c}{\partial x} = \frac{\partial}{\partial y}\left[\chi_1 \frac{\partial c}{\partial y} - v c\right] + c \frac{\partial v}{\partial y}$$

The term v is composed of two components: the fluid velocity $\underline{v}$ and the mean fall velocity V_s which equals zero for a neutrally bouyant contaminant. The velocity components, determined from a previous calculation, are considered to be constant at a particular point. The boundary conditions are, at the surface of the plate,

$$\chi_1 \frac{\partial c}{\partial y} - v c = 0$$

where no settling or absorption of the contaminant is experienced; and at $y = +\infty$, or far from the source,

$$\frac{\partial c}{\partial y} = 0 \ .$$

The boundary condition at the surface of the plate states that the net rate of supply of contaminant to the region immediately above the surface due to the turbulent mass transfer must be equally and oppositely balanced by the rate of removal due to convection. The boundary condition for $y = +\infty$, or far above the surface of the plate, states that the gradient cannot exist at the upper limit of

the field of interest. This boundary condition requires careful attention when the magnitude of the field height is determined. The field must possess a height great enough such that the plume of contaminant can never interact with the boundary.

In addition to these boundary conditions, a source condition is needed. This requires that some form of concentration distribution be established at some beginning value of x.

To provide greater flexibility toward the solution of the general mass transport problem, the turbulent diffusion equation (4) was made dimensionless by introducing the following parameters where the prime notation indicates a dimensionless quantity:

$c' = \frac{c}{c_o}$, dimensionless concentration

$x' = \frac{X}{L_x}$, dimensionless distance along the x-coordinate

$y' = \frac{y}{L_x}$, dimensionless distance along the y-direction

$t' = \frac{t\bar{\xi}}{L_x^2}$, dimensionless time (t' is x-dependent through $\bar{\xi}$)

$u' = \frac{u\ L_x}{\bar{\xi}}$, dimensionless velocity in direction of flow

$v' = \frac{v\ L_x}{\bar{\xi}}$, dimensionless velocity in the vertical direction

$\psi' = \chi_1/\bar{\xi}$, dimensionless transfer coefficient.

In the preceeding parameter list, L_x = the length of the field of interest; c_o = the maximum concentration at the source; and $\bar{\xi}$ = the depth averaged value of the eddy diffusivity for momentum transfer. The nondimensional transfer coefficient ψ' represents the ratio of mass transfer to momentum transfer and may be interpreted as the inverse of the local Schmidt number.

Substitution of the listed parameters into equation (4) yields (dropping the primed notation at this point)

$$\frac{\partial c}{\partial t} + u\frac{\partial c}{\partial x} = \frac{\partial}{\partial y}\left[\psi\frac{\partial c}{\partial y} - v c\right] + c\frac{\partial v}{\partial y} \qquad (7)$$

Equation (7) is the nondimensional turbulent diffusion equation from which the local field concentrations may be obtained with respect to the initial source concentration. In the hypothetical uniform, two-dimensional turbulent boundary layer flow, the velocity components do not vary at a point in the flow; and the concentration by volume is small.

The boundary condition at the surface of the plate becomes

$$\psi\frac{\partial c}{\partial y} - vc = 0 \quad ; \qquad (8)$$

and, in terms of nondimensional quantities, the boundary condition at $y = +\infty$ is $\partial c/\partial y = 0$. For a detailed treatment of the boundary conditions and the source condition, see

Appendix B.

In order to solve equation (7) for the field point concentration with respect to the source concentration, we must determine an expression for $\psi = \psi(x,y)$ as well as its partial derivative with respect to the boundary layer coordinate y. From our previous definition, $\psi = \chi_1/\overline{\xi}$. Here $\chi_1 = \chi + \varepsilon_y$, and $\overline{\xi} = 1/L_y \int_o^{L_y} \xi \, dy$ where $\xi = \nu + \varepsilon_m$ and L_y = the total field height. From a known velocity and shear stress distribution in a two-dimensional flow, the turbulent momentum transfer coefficient, ε_m, can be computed from Boussinesq's definition:

$$\rho \epsilon_m \frac{\partial u}{\partial y} = \tau_{xy} \tag{9}$$

in which τ_{xy} = the shearing stress acting parallel to the x coordinate on a surface normal to the y coordinate, and ρ = the fluid density. For the two-dimensional flow considered here, the shear stress distribution can be represented as

$$\tau_{xy} = \tau_w \left(1 - \frac{y}{\delta} \right) \tag{10}$$

where τ_w = the shear stress at the surface of the flat plate.

Using the logarithmic velocity profile, equation (5), in conjunction with the definition of ψ and equations (9) and (10), we have (see Appendix C)

$$\psi = \chi_1/\bar{\xi} \quad \text{for } 0 \leq y \leq \delta, \text{ and}$$

$$\psi = \chi/\bar{\xi} \quad \text{for } y > \delta. \tag{11}$$

In equation set (11),

$$\chi_1 = \chi + \frac{y u_*}{A}\left(1 - \frac{y}{\delta}\right) \tag{12}$$

and

$$\bar{\xi} = \frac{u_* \delta^2}{6 A L_y} + \nu \quad . \tag{13}$$

Using the power law form of the velocity profile, equation (6), we have $\psi = \chi_1/\bar{\xi}$ for $y \leq \delta$ when

$$\chi_1 = \chi + \frac{u_*^2 \delta}{a b U_\infty}\left(\frac{y}{\delta}\right)^{1-b}\left(1 - \frac{y}{\delta}\right) \tag{14}$$

and

$$\bar{\xi} = \nu\left[1 + \frac{u_*}{a b U_\infty}\,\frac{\delta}{L_y}\,\frac{u_* \delta}{\nu}\,\frac{1}{Q}\right] . \tag{15}$$

In equation (15), $Q = 6 - 5b + b^2$. Thus we have two approximations to the velocity field and their corresponding ψ-distributions.

With an approximate distribution for the nondimensional transfer coefficient available, the finite difference quotients for the derivatives in the diffusion equation (7) were written implicitly in both time and space where $c_{i+1,j}^{n-1}$ represents the value of $c_{i+1,j}^{n}$ at the previous time step. This formulation of the finite difference quotients required the establishment of a grid system as shown in Figure 2. The indices i and j define the location of various points with respect to the x and y axes respectively.

The development of a numerical solution of equation (7) requires the consideration of two important elements. First, at a given time the concentration c(x,y,t) at the general point (i+1,j) is influenced by all the points of region A in Figure 2. Secondly, second derivatives exist only along one coordinate in the concentration equation. Utilizing the above considerations, the partial derivatives of equation (7) were written in finite difference form and exhibit the four point relationship as illustrated in Figure 3. Thus,

$$\left.\frac{\partial c}{\partial t}\right|^{m}_{i+1,j} = \frac{c^{m}_{i+1,j} - c^{m-1}_{i+1,j}}{\Delta t_{i+1}}$$

$$\left.\frac{\partial c}{\partial x}\right|^{m}_{i+1,j} = \frac{c^{m}_{i+1,j} - c^{m}_{i,j}}{\Delta x} \qquad (16)$$

$$\left.\frac{\partial c}{\partial y}\right|^{m}_{i+1,j} = \frac{c^{m}_{i+1,j+1} - c^{m}_{i+1,j-1}}{2\Delta y}$$

$$\left.\frac{\partial^2 c}{\partial y^2}\right|^{m}_{i+1,j} = \frac{c^{m}_{i+1,j+1} - 2c^{m}_{i+1,j} + c^{m}_{i+1,j-1}}{\Delta y^2} \quad .$$

Substitution of the above finite difference quotients into equation (7) with

$$R^{m}_{i+1,j} = \left.\frac{\partial \Psi}{\partial y}\right|^{m}_{i+1,j}$$

results in the following expression,

$$
\begin{aligned}
& C^{m}_{i+1,j-1}\left[-\frac{v_{i+1,j}}{2\Delta y}+\frac{R_{i+1,j}}{2\Delta y}-\frac{\psi_{i+1,j}}{\Delta y^{2}}\right] \\
& +C^{m}_{i+1,j}\left[\frac{1}{\Delta t_{i+1}}+\frac{u_{i+1,j}}{\Delta x}+\frac{2\psi_{i+1,j}}{\Delta y^{2}}\right] \\
& +C^{m}_{i+1,j+1}\left[\frac{v_{i+1,j}}{2\Delta y}-\frac{R_{i+1,j}}{2\Delta y}-\frac{\psi_{i+1,j}}{\Delta y^{2}}\right] \\
& =\frac{C^{m-1}_{i+1,j}}{\Delta t_{i+1}}+C^{m}_{i,j}\,\frac{u_{i+1,j}}{\Delta x} \quad .
\end{aligned}
\tag{17}
$$

Letting the terms in brackets on the left hand side of equation (17) be represented by A, B, and C, respectively, and representing the right hand side by D, we may write (J-2) equations in (J-2) unknowns, for $2 \leq j \leq (J-1)$. This results in a tridiagonal matrix type system of equations which may be solved using an efficient algorithm suitable for solving such a set of equations.

For varying values of j, equation (17) may be written as

$$
\begin{aligned}
&(j=2) && B_2 c_2 + C_2 c_3 = D_2 - A_2 c_1 \\
&(3 \leq j \leq J-2) && A_j c_{j-1} + B_j c_j + C_j c_{j+1} = D_j \\
&(j=J-1) && A_{J-1} c_{J-2} + B_{J-1} c_{J-1} = D_{J-1} - C_{J-1} c_J
\end{aligned}
\tag{18}
$$

where the terms C_1 and C_J are determined from the boundary conditions, see Appendix B,

$$C_{i+1,1} = \frac{4}{3} C_{i+1,2} - \frac{1}{3} C_{i+1,3}; \text{ and } C_{i+1,J} = C_{i+1,J-1} .$$

Equation set (18) is solved using subroutine TRIDAG along the boundary layer coordinate, from the freestream to the surface of the plate, for each step in the x-direction at a given value of time.

To summarize, the computation scheme for calculation of the point concentrations of pollutant throughout the field is as follows: first, the physical dimensions of the field are established, and the local velocities at each point are determined using either of the velocity profile approximations previously discussed. In conjunction with the velocity calculations, the local values of the non-dimensional transfer coefficient and its partial derivative with respect to y is determined. Now, the solution of the concentration field remains to be obtained. After the field is initialized, the values of the concentrations throughout the field set equal to zero except at the source where a source concentration distribution is established, the boundary conditions are invoked, and the diffusion equation is evaluated along the boundary layer coordinate (y). The result is a set of simultaneous equations having a tri-diagonal matrix form. The solution of the tridiagonal matrix yields the approximate point concentrations throughout the boundary layer at x-station (i+1). The solution is repeated for all i-stations until the complete field is obtained. The concentration field is said to have converged

to the approximate steady state solution when the absolute value of the difference between the values of the concentration, at a particular point, for the current and previous time step is less than some constant, ε. The convergence criterion used in this investigation is

$$\left| c^{m}_{i+1,j} - c^{m-1}_{i+1,j} \right| \leq 10^{-4} = \epsilon$$

where n represents the number of time steps required. A provision was made in the computer program (Appendix E) to eliminate, on the current time step, that portion of the field which had converged on the previous time step. Therefore, the concentration field was effectively reduced to only two i-stations during the final time step solution. Utilization of this feature saved considerable computer time in each analysis.

The construction of a plausible procedure for obtaining the values c throughout the flow field leads to the consideration of the question of whether these values actually represent a good approximation to the solution of the original partial differential equation. Supposing as usual that c possessed a sufficient number of partial derivatives, a Taylor's expansion was written for the elements $c^{n}_{i+1,j+1}$, $c^{n}_{i+1,j}$, $c^{n}_{i+1,j-1}$, and $c^{n-1}_{i+1,j}$ in equation (17). Replacement of these terms by their Taylor's expansion and consolidation of the resulting expression resulted in a truncation error proportional to Δx, Δy^2, and Δt. Thus

the truncation error approaches zero with Δx, Δy^2 and Δt; and it is probable that the results from the implicit finite difference formulation of the diffusion equation converge to the solution of the partial differential equation as Δx, Δy^2, and Δt approach zero, provided the necessary stability criteria are considered.

A stability analysis for the numerical solution yielded the following results:

(a) No stability requirement exists in the y-direction since the equations are actually solved along the y-coordinate by a direct method.

(b) If Δy is such that K is real and negative, where

$$K = \frac{1}{\Delta t} + \frac{u}{\Delta x} + \frac{2\Psi}{\Delta y^2} + 2\left[\frac{\Psi^2}{\Delta y^4} - \left(\frac{v - \frac{\partial \Psi}{\partial y}}{4\Delta y^2}\right)^2\right]^{1/2}$$ and

$$\Delta y^2 \leq \frac{4\Psi^2}{\left(v - \frac{\partial \Psi}{\partial y}\right)^2},$$ then it is required to have

$$\Delta t < \left[-4\Psi \Delta x\right] \Big/ \left[\left(v - \frac{\partial \Psi}{\partial y}\right)^2 \Delta x + 4\Psi u\right]$$

and $\psi < 0$. This condition is physically unrealistic since $\psi \sim \varepsilon_y/\varepsilon_m < 0$ implies a negative coefficient of eddy diffusivity.

(c) Other than the stability condition established in (b) above, the numerical solution is stable for all cases where

(1) K is real and greater than zero; with

$$\Delta y^2 \leq 4\Psi^2 \Big/ \left(v - \frac{\partial \Psi}{\partial y}\right)^2$$, and $\Delta t > 0$

(2) K is complex and either positive or negative;

with $\Delta y > 2\psi/\left(v - \frac{\partial \psi}{\partial y}\right)$, and $\Delta t > 0$.

No stability problems were encountered in any of the computer runs used in this investigation.

For a more detailed description of the stability analysis, see Appendix D.

V. DISCUSSION OF THE EXPERIMENTAL PROBLEM

To verify the results of the numerical solution of the diffusion equation, several computer runs were made to model an experiment dealing with the diffusion of gaseous ammonia from a line source on the surface into the turbulent boundary layer over a flat plate. The experiments were conducted in a noncirculating wind tunnel located in the Fluid Dynamics and Diffusion Laboratory of Colorado State University [19]. The test section was approximately 80 feet long and 6 x 6 feet square, slightly increasing in width in the direction of the flow to provide a zero longitudinal pressure gradient.

Three ambient velocities of 9, 12, and 16 ft./sec. were used in the experiment. Mean velocities were measured by a manually balanced, constant temperature, hot-wire anemometer. The mean velocity profiles within the test section were approximately similar and were fitted to the one-seventh power law formula, see Figure 2 of Poreh and Cermak [9]. The boundary layer thickness δ varied from 5 to 11 inches. (The boundary layer thickness was taken to be the vertical height at which $u = 0.99\ U_\infty$.) The Reynolds number $U_{amb}\ (\delta/\nu)$ varied from 25,000 to 56,000, and the boundary layer was turbulent throughout the entire test range.

Anhydrous ammonia gas (NH_3) was emitted from a line source located on the plate surface. The molecular diffusivity of ammonia at 25°C is $\chi = 0.236$ cm^2/s. Samples of the air-gas mixture were taken using a chemical gas analyzer, and air-gas withdrawal rates were adjusted to approximately the local velocity of the air stream except, of course, near the surface. The minimum sampling time was one minute, but the usual sampling time was between 2 and 3 minutes. The sampled air-gas mixture was passed through an absorption tube containing dilute hydrochloric acid which absorbed the ammonia. The absorbed ammonia was then chemically treated. The absolute quantities of ammonia were determined with a photo-electric colorimeter.

A large number of samples were taken, and a standard deviation of up to 6 percent was encountered between separate readings of standard solutions taken at different times using different preparations of Nessler's Reagent. The colorimetric method was not accurate where very mild concentrations were involved. This influenced the recorded concentrations near the upper edge of the plume.

The data for the experiment were reproducible within a deviation of 10 percent between averages of different runs on different dates. Better data were obtained close to the source in the Series I tests described below. The above estimation of the error does not include the upper edge of the plume which was less than 15 percent of the maximum surface concentration and very small in its absolute value.

Two series of experiments were conducted. In each series three ambient velocities were used—9, 12, and 16 ft./sec. In Series I, the source was located on the plate surface at a station X = 33.5 feet downstream of the leading edge of the flat plate. Measurements were taken at numerous heights through the boundary layer for stations 3, 5, 9, 15, and 21 feet downstream from the source. Data from the Series I and Series II tests established the existence of quasi-similar concentration profiles which divided the flow field into zones designated as "intermediate," "transition," and "final," see Figure 7. The Series I tests provided concentration profiles which were categorized in the intermediate and transition zones. The mass flux of ammonia per unit width in the Series I tests was G = 0.66 mg/cm·s.

In the Series II tests, the source was located at a station 15.5 feet downstream of the leading edge of the plate. Measurements were taken at 17, 23.5, 35.5, and 43.5 feet downstream from the source thus extending into the final zone. The mass flux of ammonia per unit width in the Series II tests was G = 0.55 mg/cm·s.

A relative rate parameter β was used to assist in dividing the field downstream from the source into the zones and in considering the effect of the non-homogeneous turbulence of the flow field on the diffusion process.

A characteristic length to give an indication of the rate of change of growth of the boundary layer was defined

as $L_\delta = \delta/(d\delta/dx)$. A similar length was defined to express the rate of change in the diffusion process. With λ equal to a characteristic height of a region contaminated by the ammonia, and $c/c_{max} = f(\alpha)$ where $\alpha = y/\lambda$, we define $f(1) = 0.50$. Therefore we may write $L_\lambda = \lambda/(d\lambda/dx)$, and the ratio $\beta = L_\lambda/L_\delta$ is a measure of the relative rate of growth of the plume and the momentum boundary layer. The experimental data [9] were characterized into zones with the following approximate limits:

intermediate zone: $\beta \leq 0.4$,

transition zone: $0.4 < \beta \leq 0.85$, and

final zone: $\beta > 0.85$ and approaches a constant value of 1.00.

The preceeding discussion of the experiment was paraphrased from reference [9]. In this investigation the experimental data from [9] is considered adequate to verify the results of the numerical solution of the diffusion equation.

VI. COMPARISON OF EXPERIMENTAL AND PREDICTED RESULTS

The experiment discussed in the previous chapter was modeled using the computer solution of the diffusion equation. The tests for both Series I and Series II were modeled using an ambient velocity of U_∞ = 9.0 ft./sec. for a neutrally bouyant contaminant. The assumption of neutral bouyancy was taken as an engineering approximation to the problem; while in the actual experiment, the ammonia was slightly bouyant due to the density differences existing between the contaminant and the main flow of air. The one-seventh power law was used to approximate the velocity profiles in the wind tunnel, as stated in the previous chapter.

Figure 4 presents a comparison between the calculated and measured boundary layer thickness along the test section for ambient velocities of 9 and 12 feet/second. The remaining comparisons of predicted and experimental data will be made only for an ambient velocity of U_∞ = 9 ft./sec. The calculated boundary layer thickness is slightly greater than that encountered in the experiment; however, as seen from Figure 4(a) and 4(b), the rate of growth of both the calculated and measured boundary layers is the same.

Figure 4 indicates the use of two values of the variable NSIY, where NSIY represents the desired number of intervals Δy inside the boundary layer at the trailing edge of the concentration field. This variable exerts no influence upon the boundary layer thickness. Using this variable one can alter the step size, Δy, which in turn alters the magnitude of the vertical dimension of the flow field.

Figure 5 presents the boundary layer thickness for distances downstream of the source. Hence, the rate of growth of the boundary layer for a particular test series can be compared to the rate of growth of the plume of pollutant, Figure 6, for corresponding source locations.

Figure 6 compares the experimentally determined characteristic plume height with the predicted value in the intermediate zone for the Series I tests. The predicted characteristic plume thickness for the Series II tests is also shown, and good agreement between the various sets of data is observed. Note that for a given x-distance downstream from the source, the plume thickness for the Series I predictions is greater than that for the Series II predictions. This difference is due simply to the variation in the source position relative to the leading edge of the plate and hence to the variation in the boundary layer thickness for a given distance downstream of the source. Thus the importance of the relative rate parameter β, with respect to the establishment of the zones of similarity for the concentration profiles, is implied. The fact that β is

not a universal function is clearly illustrated in Figures 10 and 11.

The predictions of the characteristic plume height for the Series I tests agree well with the measured parameter from a distance of about 60 cm. downstream of the source. The predictions for the Series II tests are also very reasonable. However, within about 40 cm. of the source, the predictions do not provide very meaningful values of λ for either series of tests. This divergence from the measured plume thickness near the source is believed to be due to one or a combination of the following: (a) the longitudinal concentration gradients are not initially small, see Figures 15 and 16, and (b) the concept of a gradient type eddy diffusivity coefficient is not known to be valid until the plume thickness is relatively large compared to the eddies causing the transfer. The data in Figure 6 implies that a larger number of steps (smaller Δy) taken inside the boundary layer provides a better agreement between the predicted and measured values of the characteristic plume thickness.

For a sufficiently large distance downstream of the source, satisfactory agreement between the predicted and measured value of the characteristic plume thickness has been established. Now we consider the concentration profiles characteristic of each zone and compare the predicted profiles with those obtained by experiment.

Figure 7 presents the experimental concentration profiles encountered in the intermediate and final zones. Mean or average profiles were drawn to depict a characteristic shape of the profiles within a particular zone. Note the shift in the curvature of the profile as the plume proceeds downstream of the source through the intermediate zone to the final zone. For the final zone, the mean experimental profile was determined under the conditions of Series II tests in which the source was moved closer to the leading edge of the plate. There was considerable scatter in the experimental data taken in the final zone. This scatter was probably due to the low absolute values of the concentration near the edge of the plume so far from the source.

Figure 8 compares the experimental and predicted concentration profiles for the Series I tests only. Data for two values of NSIY are presented. Both profiles, (a) and (b), contain data which extends through the intermediate zone and into the transition zone. Excellent agreement between the predicted and measured profiles is observed. This implies the validity of the use of boundary layer type approximations in the establishment of the final form of the diffusion equation, except near the source. Also the assumption that the pollutant was neutrally bouyant seems well founded. In the intermediate zone, the longitudinal gradients in the concentration field are small compared to the vertical gradients.

The ratio β is small, and the diffusion process does not seem to be greatly affected by the rate of growth of the boundary layer [9].

A comparison of experimental and predicted concentration profiles, for two values of NSIY, for the Series II tests is presented in Figure 9. Note that as the value of x, the distance downstream of the source, increases, the predicted profiles shift from the intermediate zone profile to that detected in the final zone. The deviation between the experimental and predicted curves experienced here may be related first to the assumption of a neutrally bouyant pollutant and secondly to a discontinuity in the slope of the distribution of the nondimensional transfer coefficient which will be discussed later, see Figure 14. The error introduced by the assumption that the ammonia gas was neutrally bouyant appears to be most evident as the plume approaches the final zone in its diffusion process. The introduction of a positive (upward) mean fall velocity tends to decrease the deviation between the calculated and measured diffusion parameters. Simultaneously consider Figures 9, 12, and 13 with Table II. Figure 9 shows that with an increasing distance downstream of the source the predicted concentration profiles indicate a trend to merge with the mean experimental profile. Figure 13 indicates that, as the experimental plume of the Series I tests approaches the final zone—$\lambda/\delta \approx 0.6$, the predicted ratio of

plume thickness to boundary layer thickness is somewhat less than that encountered experimentally. Therefore the lack of emphasis in the curvature of the predicted concentration profiles of Figure 9 is due in part to the fact that the simulated plume has not yet acquired the complete characteristics of the final zone as experienced by the experimental ammonia plume. The addition of an artificial bouyancy effect, $V_s > 0$, increases the ratio λ/δ of the simulated plume as the final zone is approached, see Table II. This would provide better agreement between the predicted and observed concentration profiles of the final zone. The preceeding results indicate that the particular zones may have flexible boundaries. Also, the profiles characteristic of each particular zone may vary slightly according to the physical problem at hand.

Figures 10 and 11 compare the rate of growth of the plume thickness with dimensionless functions of the boundary layer thickness. The experimental data indicated that in the final zone β asymptotically approached a constant value of 1.0, see Figure 13. Similarly, the value of λ/δ should approach a constant value of about 0.60. The final value of β calculated for the final zone agrees with that obtained from experiment. However, λ/δ approaches a constant value slightly less than that encountered in the experiment. This is due to the fact that the calculated value of δ was larger than that measured, while the calculated value of λ was

slightly less than that obtained from experiment.

Figure 13 compares the experimental and predicted values of the relative rate parameter β for a nondimensional distance downstream of the source, see Figure 12. Good agreement is shown in the intermediate and final zone; while near the source, the two curves, β, diverge.

Figure 13 also compares the experimental and calculated values of the ratio λ/δ as a function of a dimensionless distance downstream of the source. The deviation between the experimental and predicted values of λ/δ has been previously discussed.

As a whole, the comparison of the experimental data to the results predicted by the numerical solution indicated good agreement between the two, especially in the intermediate zone. An extension of the analysis of the experimental and simulated data for the Series I tests is presented in Figure 14. This figure illustrates the dependence of the nondimensional transfer coefficient ψ upon the boundary layer thickness and the distance downstream of the source. Near the source, $\lambda/\delta \approx .162$, the local value of ψ increases with the vertical distance through the plume and provides for the rapid growth of the plume near the source. As the plume grows to the approximate thickness of the boundary layer, the local value of ψ near the upper edge of the plume decreases. At this point λ/δ approaches a constant. Figure 14 clearly illustrates the inadequacies of models of

atmospheric diffusion processes which consider a variation in the mass diffusion coefficient with height only; since the local value of ψ is also a function of the distance from the source.

The abrupt change in the slope of the ψ-distribution as the plume begins to interact with the edge of the boundary layer has a definite effect on the concentration profiles in the final zone. This abrupt change in the ψ-distribution limits the effectiveness of the smooth intermittency cut-off which should extend through the edge of the boundary layer. Thus, far downstream from the source, the constant value of $k(y) = 1$ restricts the generality of the numerical solution, see Appendix C. However, acknowledging the slope discontinuity in the ψ-distribution curve, the numerical solution readily describes the physical characteristics of the diffusion process within the two regions of interest, the turbulent boundary layer and the adjacent free stream flow.

VII. ANALYSIS OF SEVERAL DIFFUSION PROCESSES AS MODELED BY THE NUMERICAL SOLUTION

A more general appreciation for the problem of mass diffusion in a turbulent boundary layer may be obtained from a study of Figures 15 and 16. The physical properties of the flow field are those of the Series I tests. These figures define lines of constant concentration as a plume is convected downstream of the source. The field length is 39.92 feet, the field height is 1.38 feet, the distance from the leading edge of the plate to the field is 30.08 feet, and U_∞ = 9 ft./s. In Figure 15 the source is located on the surface. Note that the region of maximum concentration is located immediately above the surface where the horizontal and vertical components of velocity are a minimum. The changes in the rate of growth of the plume are also evident, i.e., $d\lambda/dx$ is inversely proportional to the distance downstream of the source. The maximum concentration changes in the x-direction are large near the source and become gradual at some distance downstream of the source.

In Figure 16 the properties of the flow field are identical to those of Figure 15. The only difference is that the source is moved away from the surface. The maximum concentration at x-stations downstream of the source

decreases rapidly as x increases. This is attributed to the fact that the source is located near the point of maximum ψ, a region of high turbulence. Thus the contaminant quickly diffuses throughout the boundary layer. Once the plume reaches the edge of the boundary layer, the rate of growth decreases and becomes approximately equal to the rate of growth of the boundary layer. As the greater horizontal velocities in the upper region of the boundary layer tend to sweep the contaminant downstream, the line of maximum concentration descends toward the surface of the plate. The vertical position of the maximum concentration line inside the boundary layer is highly dependent upon the magnitude of the local vertical component of velocity and is thus dependent upon the lateral as well as the vertical position of the source in the flow field.

Figure 17 presents a comparison between the solutions derived from both the logarithmic and power law approximations to the velocity profiles. The diffusion problem to which the solutions were applied is that of ammonia injected into a turbulent boundary layer over a flat plate. The physical properties of the problem are as follows: L_x = 0.5 feet, the leading edge of the field is 2.0 feet downstream of the leading edge of the plate, U_∞ = 5 feet/s., V_s = 0.0 feet/s., χ = 0.000254 $ft^2/s.$, and X_T = 2.5 feet and represents the distance from the leading edge of the plate to the trailing edge of the concentration field. The source is located 2.04 feet downstream of the leading edge

of the plate. The source was located above the surface of the plate such that the ratios $y/\delta|_{source}$ for each solution were approximately equal. This allowed a more direct comparison of the ability of each solution to describe the diffusion process and eliminated the necessity of comparing the ability of each velocity profile approximation to accurately predict the boundary layer thickness over the plate. Dimensionless concentration profiles as functions of y/δ are presented for two stations downstream of the source. In both cases, the logarithmic approximation predicted the greater maximum concentration in the plume, as well as a narrower plume thickness. Both solutions indicate that the point of maximum concentration for a particular station along the plate descends toward the surface. The general shape of the concentration profiles from the two solutions indicate good comparison between the two. However, the power law approximation is the superior of the two solutions. The logarithmic approximation possesses two handicaps with respect to the simulation of the diffusion problems of Poreh and Cermak [9]. First it is limited in its ability to accurately predict the velocity profiles and boundary layer thicknesses for flows of large Reynolds numbers. Secondly, the numerical solution based on the logarithmic velocity profile approximation predicted plume thicknesses which were less developed than those predicted by the one-seventh power law simulation.

The preceding comparison illustrates the fact that the present method of solution may be applied to various approximations of the velocity profiles for the flow field. However, some relation between the particular velocity profile approximation and the particular diffusion problem to be investigated must be established before good results can be expected.

Now, reconsider the numerical solutions for the Series I tests. Table I illustrates the effect of an artificially induced vertical velocity component upon the rate of growth of the plume and hence on the relative rate parameter β. For a slightly bouyant contaminant, the magnitude of β decreases due to an increase in $d\lambda/dx$. This increased rate of growth of the plume is evident from an increase in the magnitude of the ratio λ/δ, see Table II. Thus β is also an indicator of the effects which local vertical velocity components would have on the diffusion process.

VIII. CONCLUSIONS AND REMARKS

Using the concept of eddy diffusivity and an analogy between mass and momentum transport in a turbulent boundary layer, a numerical solution of the turbulent diffusion equation was developed, and its results were compared to the experimental evidence of Poreh and Cermak [9]. Also, several other diffusion problems were investigated on the basis of the numerical solution.

From the results presented earlier, several conclusions can be specifically stated as follows:

(1) In the ammonia diffusion experiments [9] the observed shape of the quasi-similar concentration profiles in the "intermediate" and "final" zones together with the predicted profiles from the numerical solution establish the applicability of the concept of eddy diffusivity toward the solution of mass diffusion problems. The ultimate test of the suitability of the eddy diffusivity to solutions of the diffusion equation is the degree to which it predicts the concentration profiles. Good agreement between measured and predicted concentration profiles was experienced in this investigation with the velocity profiles being simulated locally by the power law formula.

(2) The numerical solution provided a good approximation to the rate of growth of the plume thickness. The

deviation of the predicted data from that taken from the experiment in the region close to the source cannot be condemned since "Very large velocity and concentration gradients made it impossible to obtain reliable data close to the source" [9].

(3) Within the "intermediate" zone, the plume is totally submerged in the boundary layer. Here the rate of growth of the plume is large compared to the rate of growth of the boundary layer. Therefore, the diffusion pattern is affected only slightly by the boundary layer changes in the zone; and as seen from Figure 14, the local value of the nondimensional transfer coefficient plays a dominant role in the overall diffusion process.

(4) Recalling that the "intermediate" zone can be regarded as an approximate model for atmospheric diffusion from a ground source in the absence of bouyancy forces, one concludes from the data presented in Figures 14, 15, and 16 that a description of the ability of the atmosphere to diffuse matter in terms of mass eddy diffusivity coefficients varying only with height is incomplete and misleading.

(5) Near the source on the plate surface, the laminar sublayer has a small effect upon the rate of growth of the plume. However, dominant elements in the diffusion process consist of the magnitude and slope of the nondimensional transfer coefficient.

(6) The concentration profile characteristics in the final zone are governed essentially by a large diffusivity

throughout the core of the turbulent layer in conjunction with a smooth intermittency cut-off as the outer edge of the boundary layer is approached from within.

(7) The boundary layer approximations and the Reynolds analogy, $\varepsilon_y = k(y)\ \varepsilon_m$ where $k(y) = 1$, may be used to describe the turbulent diffusion process within the "intermediate" zone. Good results are also obtained using these approximations in the "final" zone. However, a refinement is required for the description of the diffusion in the "initial" zone, close to the source, where the longitudinal concentration gradient is not small. Diffusion in this region is indicated to be dependent upon the existence of smaller, localized eddies near the source. As the plume grows, the importance of these smaller eddies diminishes, and the diffusion process becomes dominated by the larger eddies of the flow field.

(8) The basic numerical model developed in this investigation constitutes an efficient tool which adequately describes the diffusion processes present in a turbulent boundary layer for sources on the surface as well as for those sources above the surface.

An important feature of the numerical solution lies in its flexibility to consider the effects of various formulations of the mass eddy diffusivity coefficient upon the diffusion process as a whole. The construction of the solution with its associated computer program provides for

its adaptation, with considerable ease, to other diffusion processes of interest, in particular those which require only the modification of such elements as the boundary conditions or velocity profile simulations. When various diffusion problems are considered, it should be kept in mind that the chosen approximation to the local velocity field should be compatible with the diffusion process as a whole. That is, postulates concerning the eddy diffusivity for scalar fields with a history of development different from that of the carrier turbulent field may lead to misleading engineering results unless supported by additional information concerning the behavior of these fields.

ABSTRACT

James W. Dow, Master of Science, January, 1972

Major: Aerospace Engineering, Department of Aerophysics and Aerospace Engineering

Title of Thesis: A Direct Numerical Method for Predicting Concentration Profiles in a Turbulent Boundary Layer Over a Flat Plate

Directed by: Dr. Richard Forbes

Pages in Thesis, 105. Words in Abstract, 68.

ABSTRACT

A numerical solution of the turbulent mass transport equation utilizing the concept of eddy diffusivity is presented as an efficient method of investigating turbulent mass transport in boundary layer type flows. A Fortran computer program is used to study the two-dimensional diffusion of ammonia, from a line source on the surface, into a turbulent boundary layer over a flat plate. The results of the numerical solution are compared with experimental data to verify the results of the solution. Several other solutions to diffusion problems are presented to illustrate the versatility of the computer program and to provide some insight into the problem of mass diffusion as a whole.

*Source may be located on the surface

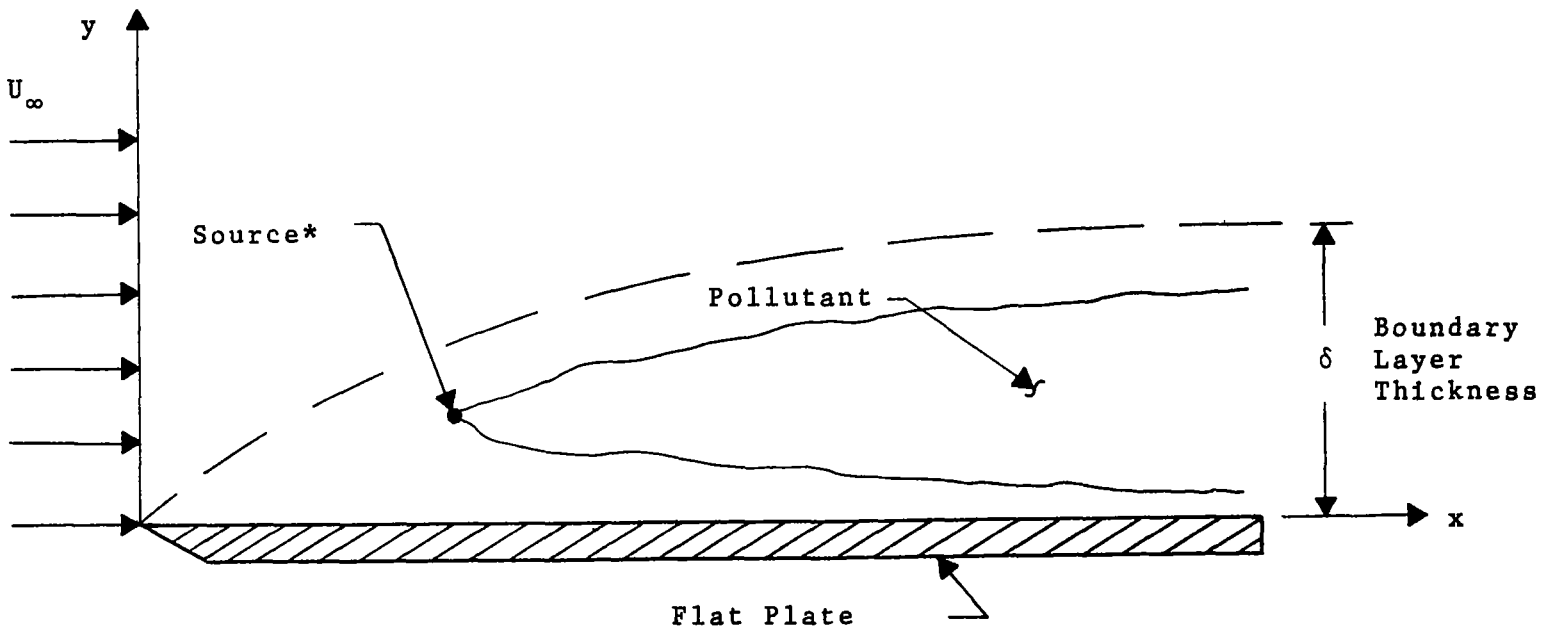

Figure 1. Definition of Coordinate System

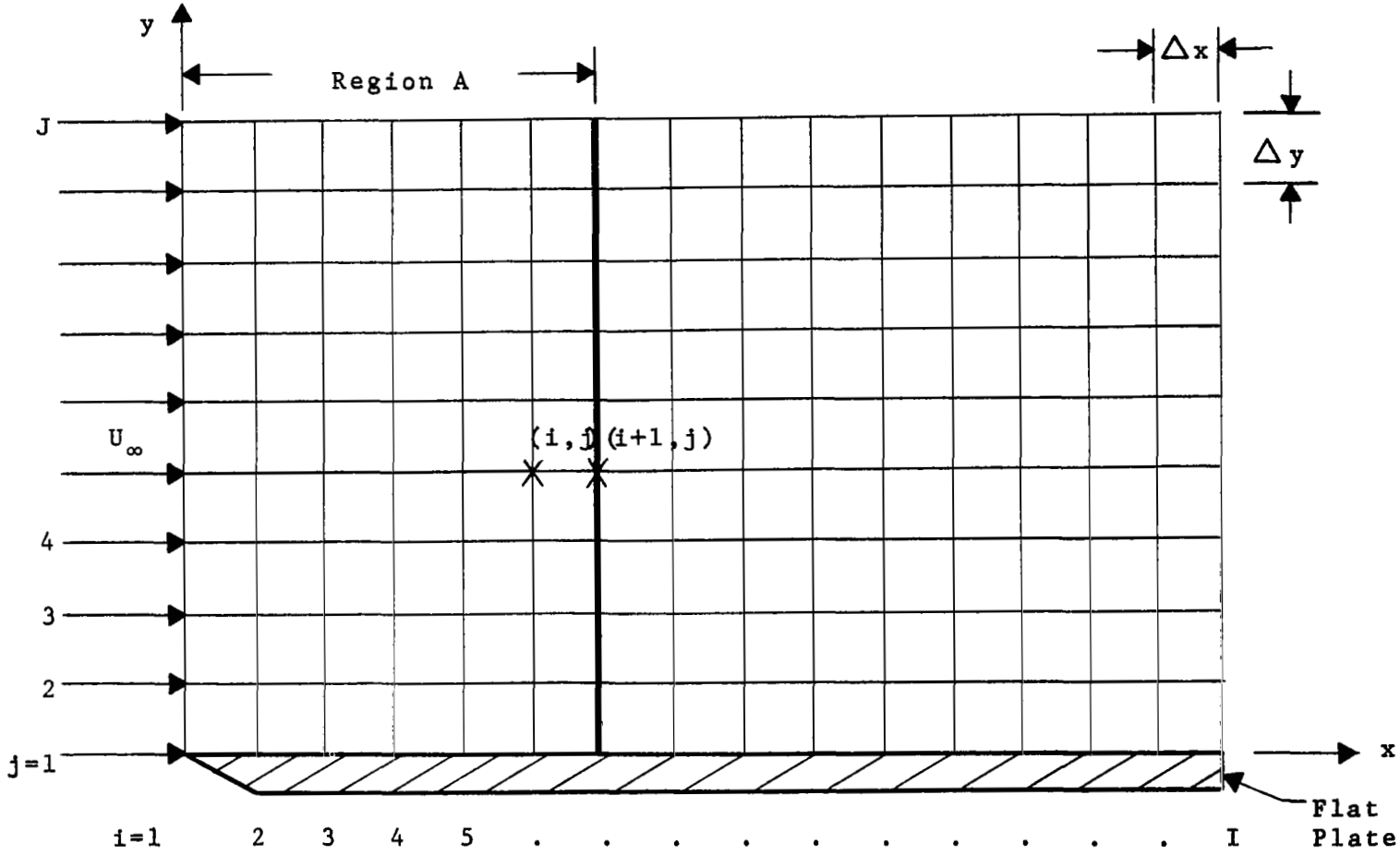

Figure 2. Two Dimensional Boundary Layer Grid System

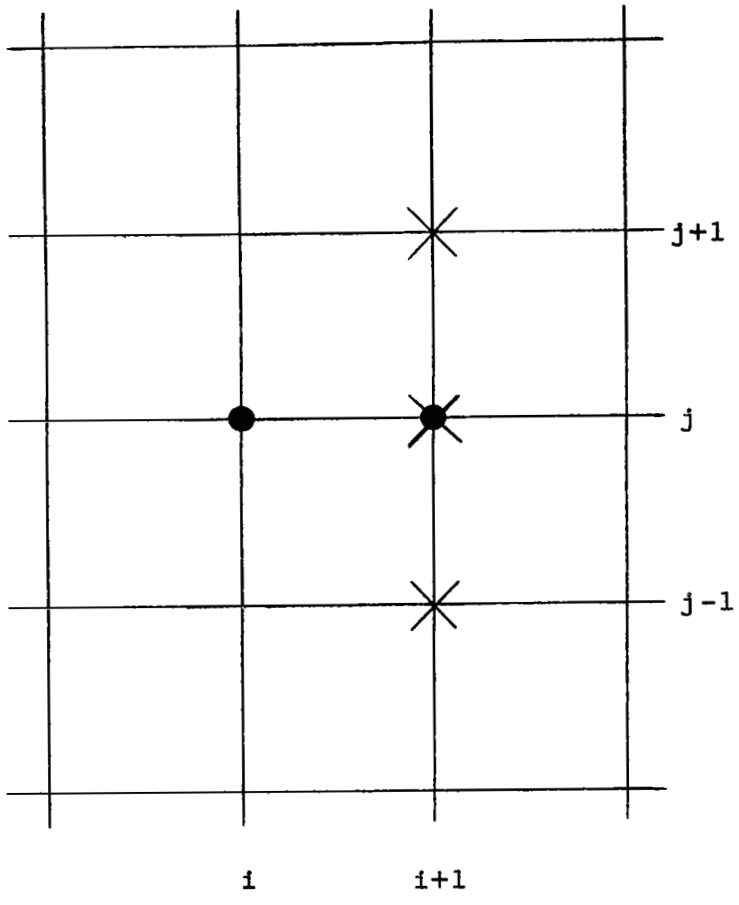

Figure 3. Relation Between Points for Implicit Formulation of Finite Difference Equations

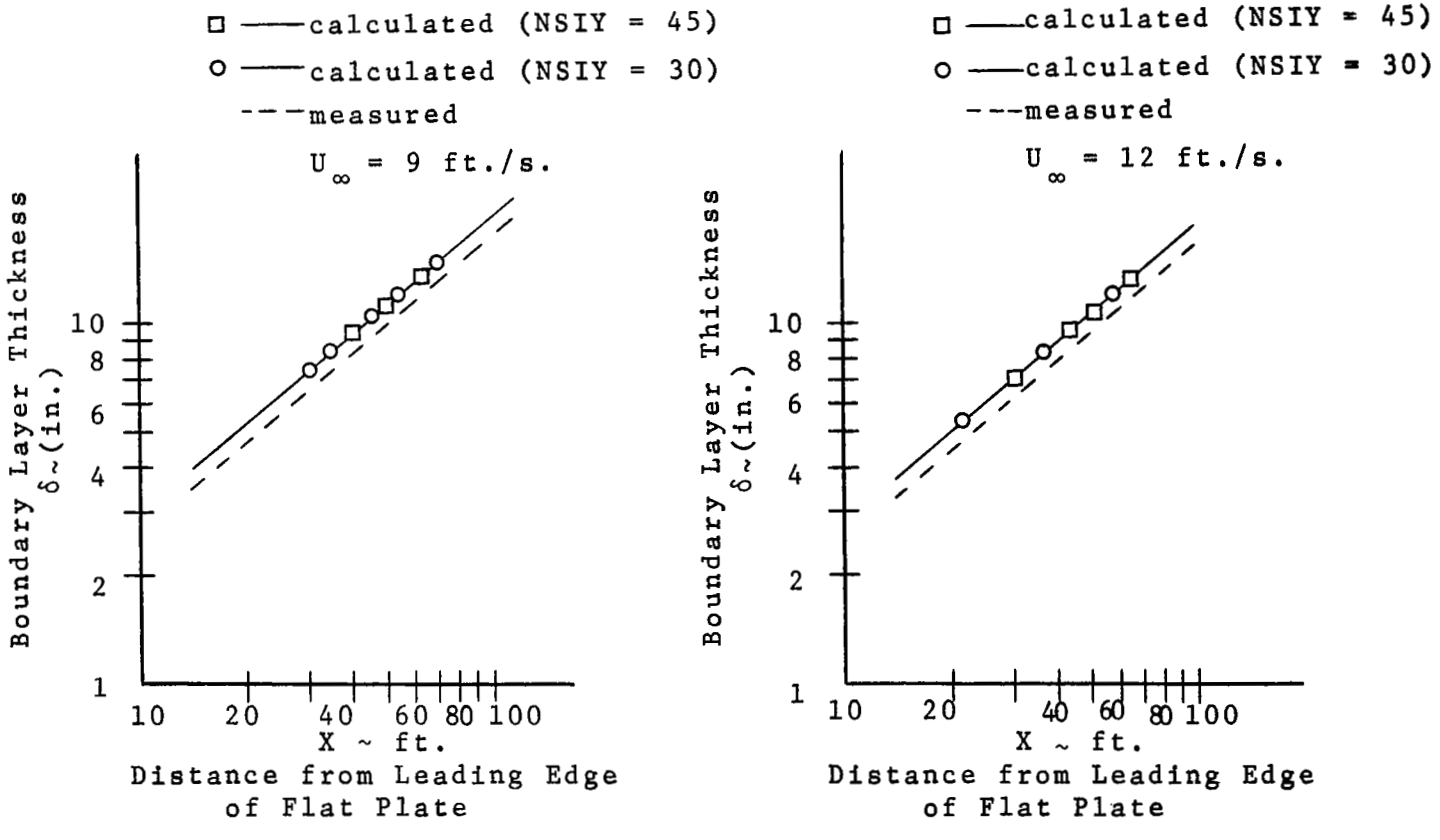

Figure 4. Comparison of Predicted and Measured Boundary Layer Thickness

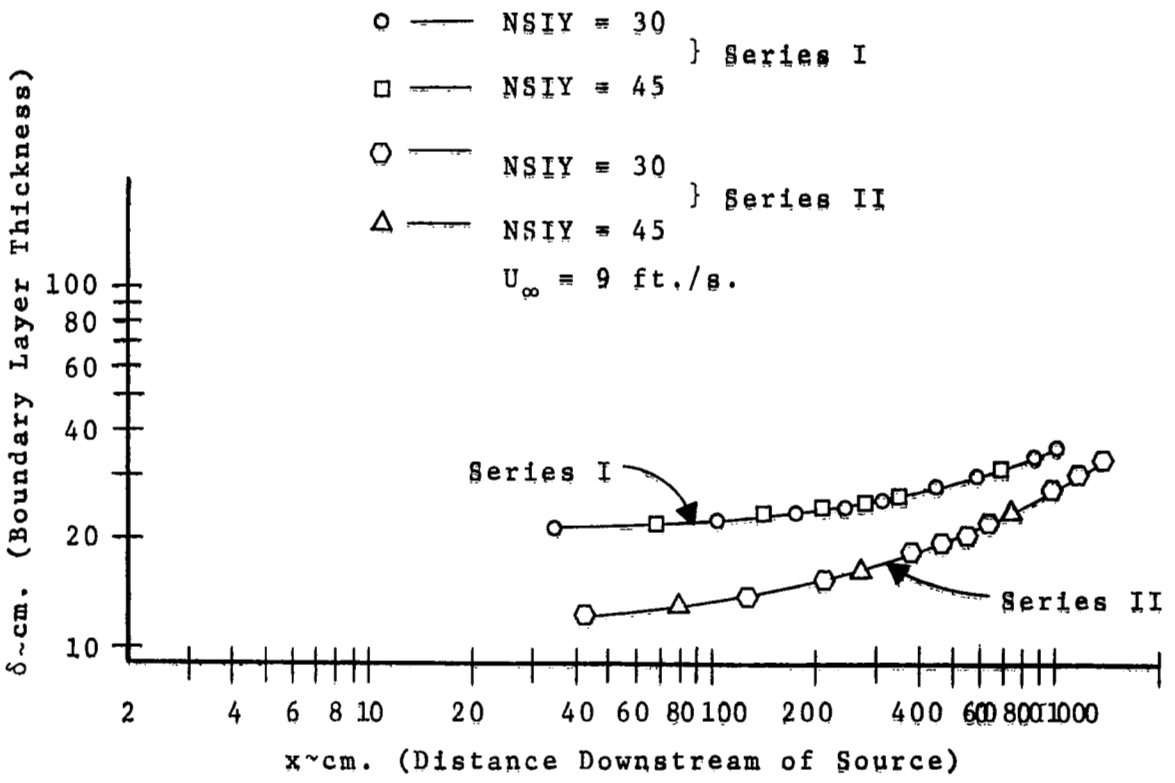

Figure 5. Predicted Growth of Boundary Layer Downstream of Source

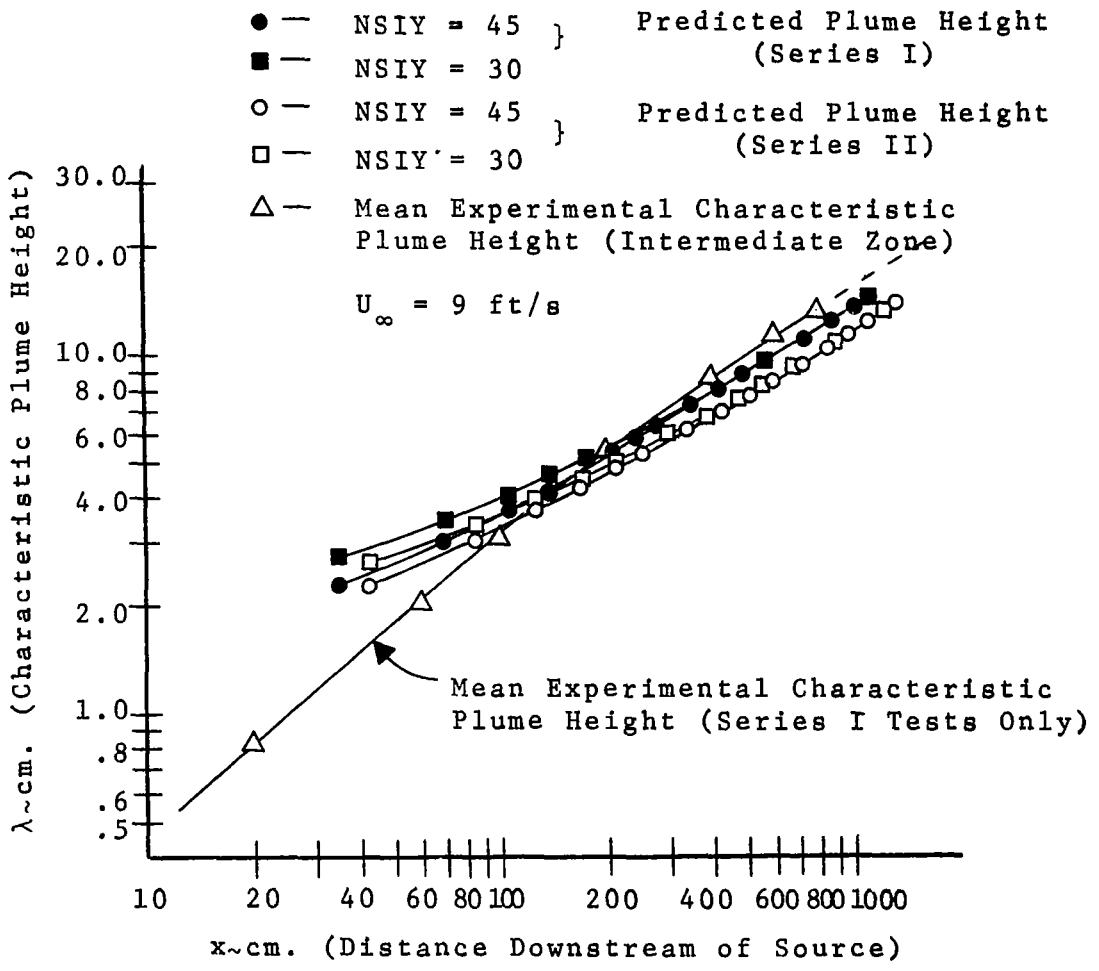

Figure 6. Comparison of Predicted and Measured Plume Thickness

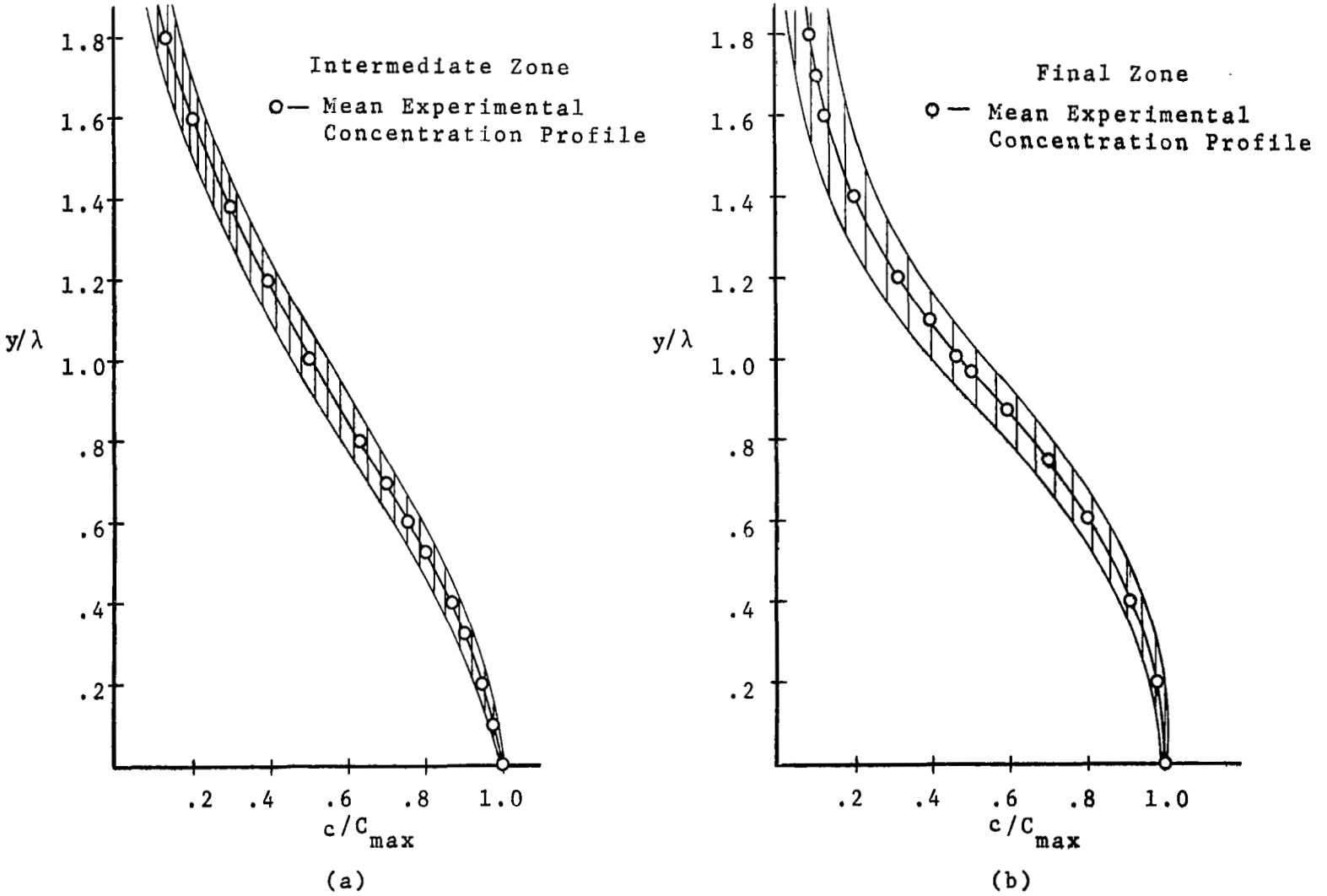

Figure 7. Quasi-Similar Experimental Concentration Profiles

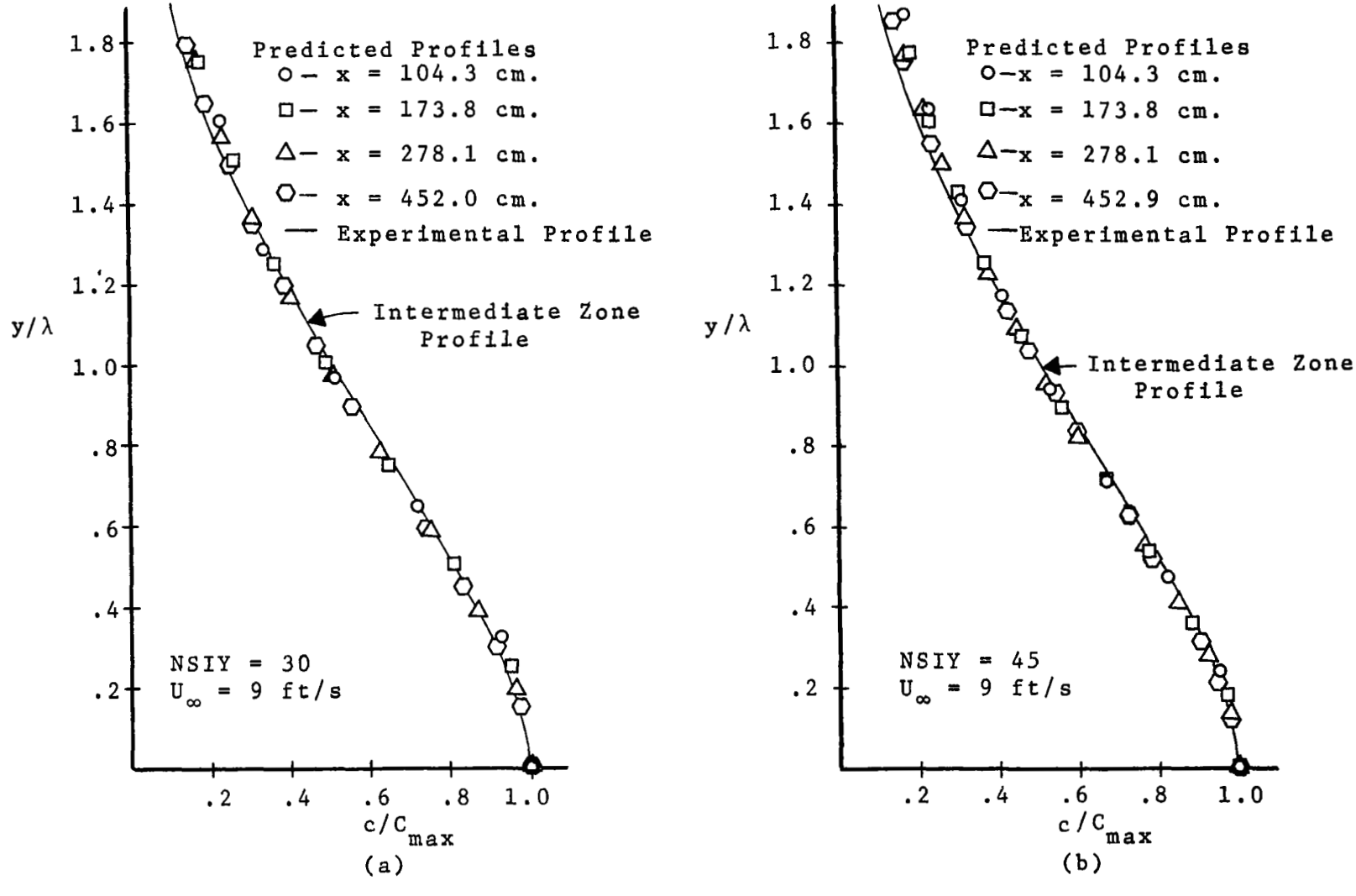

Figure 8. Comparison of Predicted and Measured Concentration Profiles for Series I

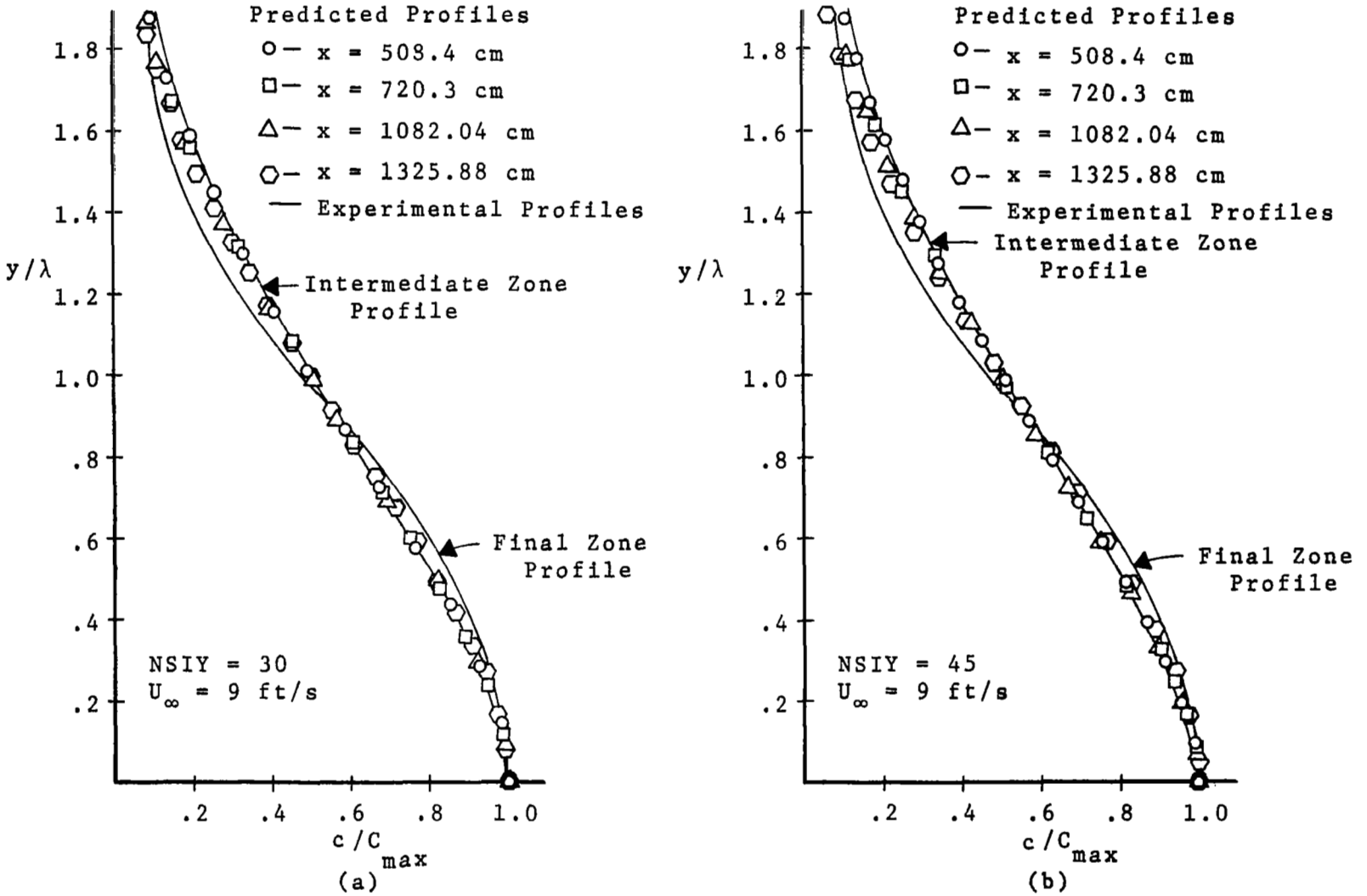

Figure 9. Comparison of Predicted and Measured Concentration Profiles for Series II

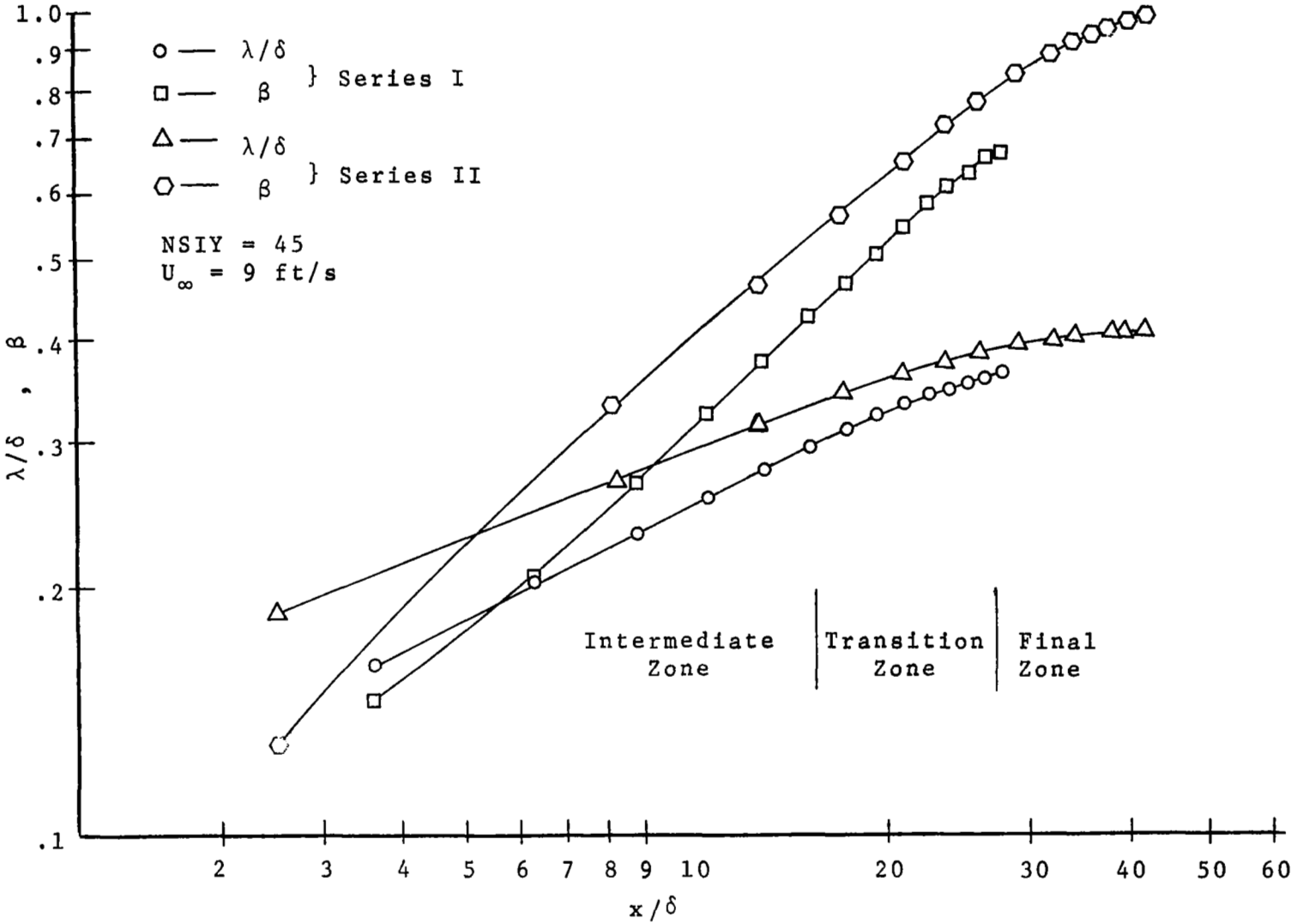

Figure 10. Relations Between Plume Growth Parameters and Distance Downstream of Source

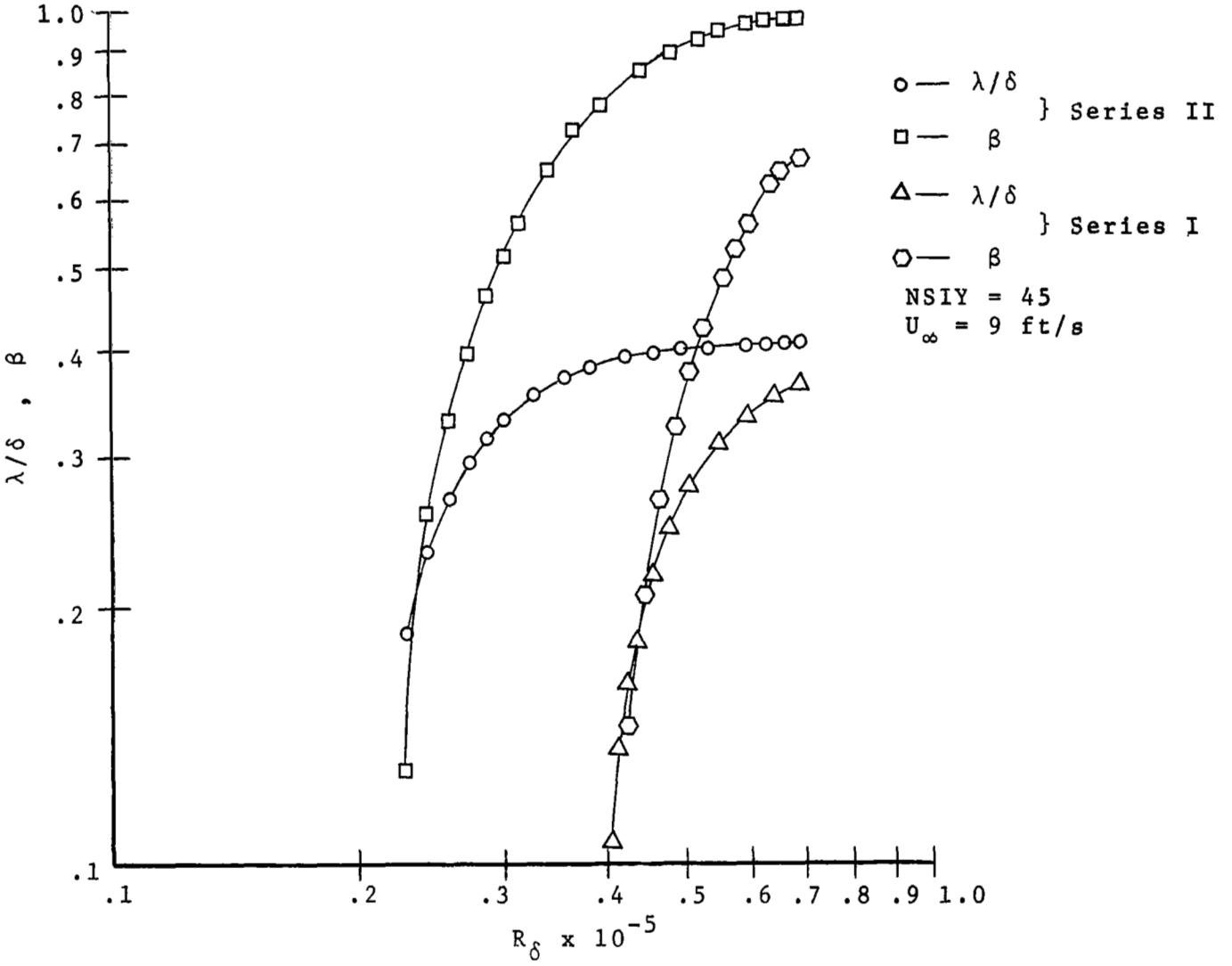

Figure 11. Variation of Plume Growth Parameters with the Reynolds Number Based on δ

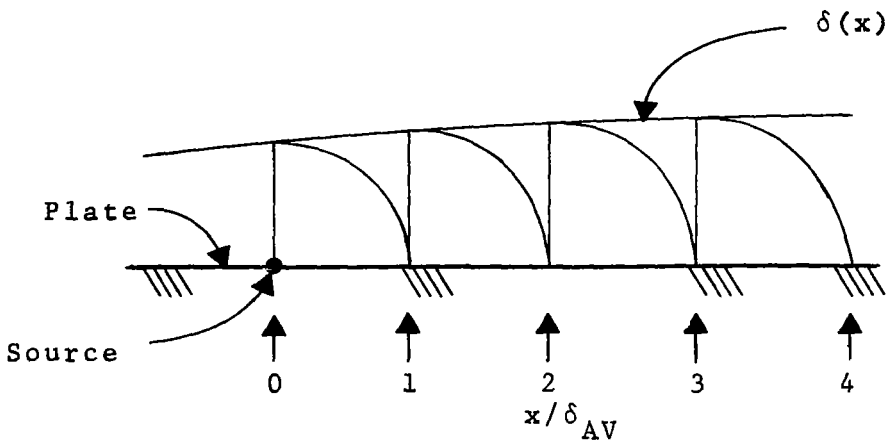

Figure 12. Determination of (x/δ_{AV})

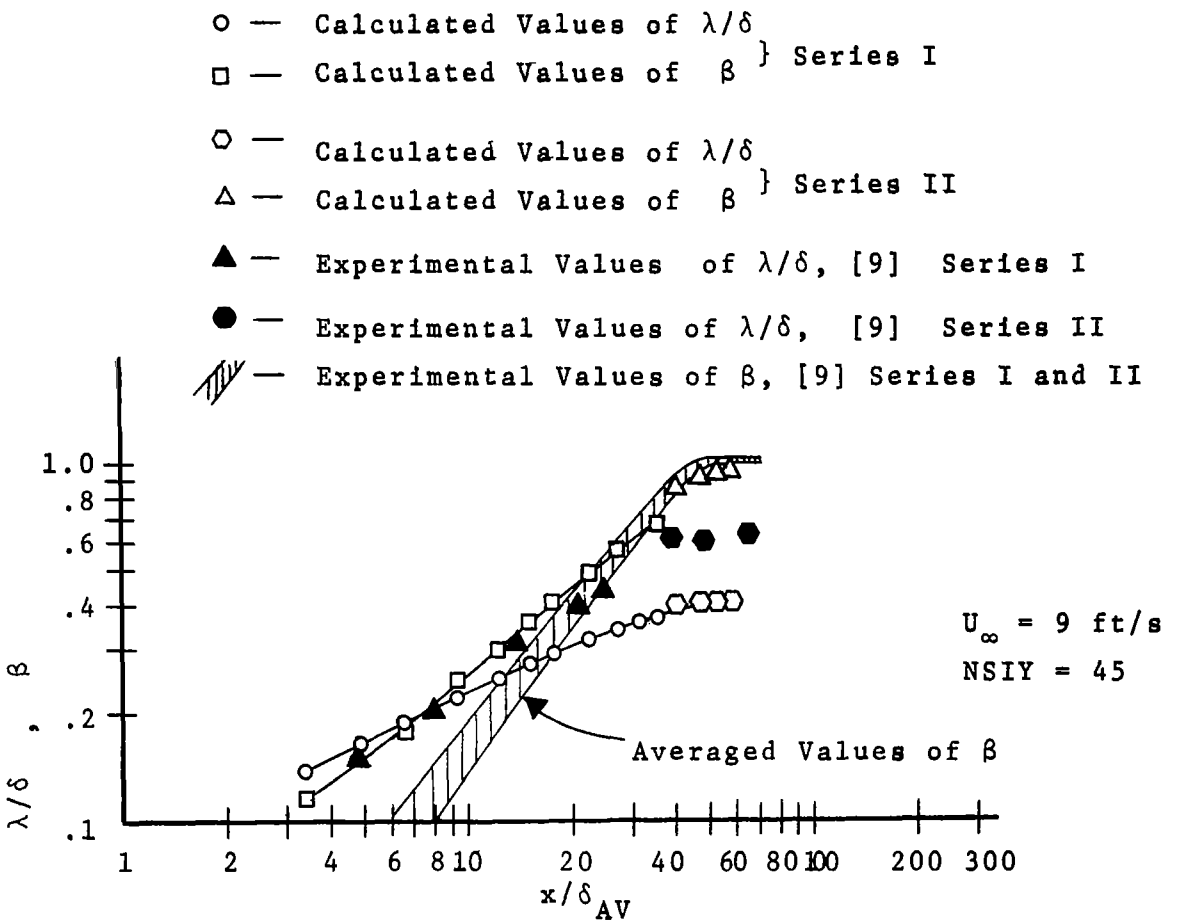

Figure 13. The Variation of (λ/δ) and β With (x/δ_{AV})

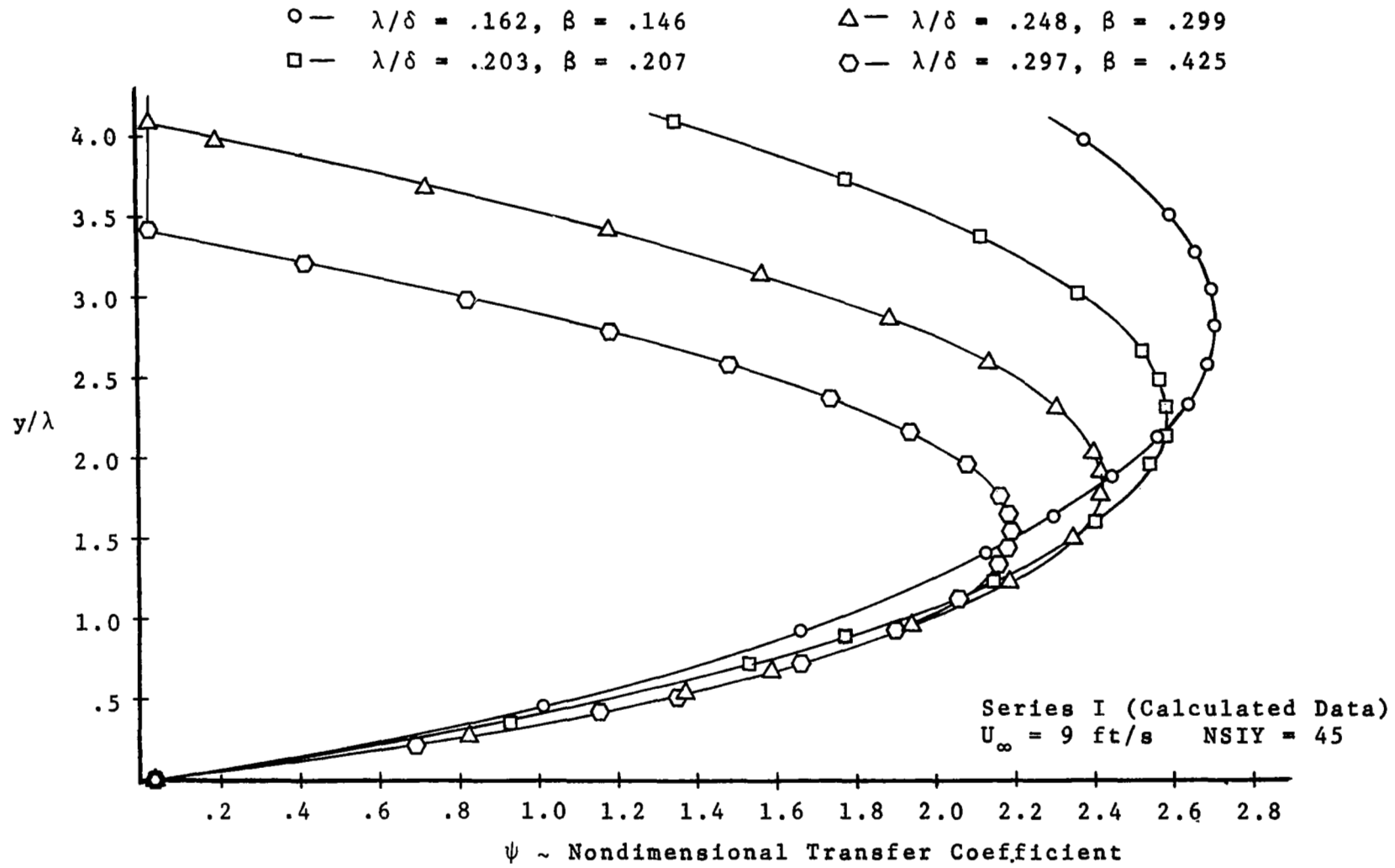

Figure 14. The Dependence of Plume Growth upon the Local Value of the Nondimensional Transfer Coefficient

Source Location: $X/X_T|_s = 0.4786$, $y/L_Y = 0.00$

Field Length = 39.93 ft XSTART = 30.08 ft.

Field Height = 1.38 ft. NSIY = 45

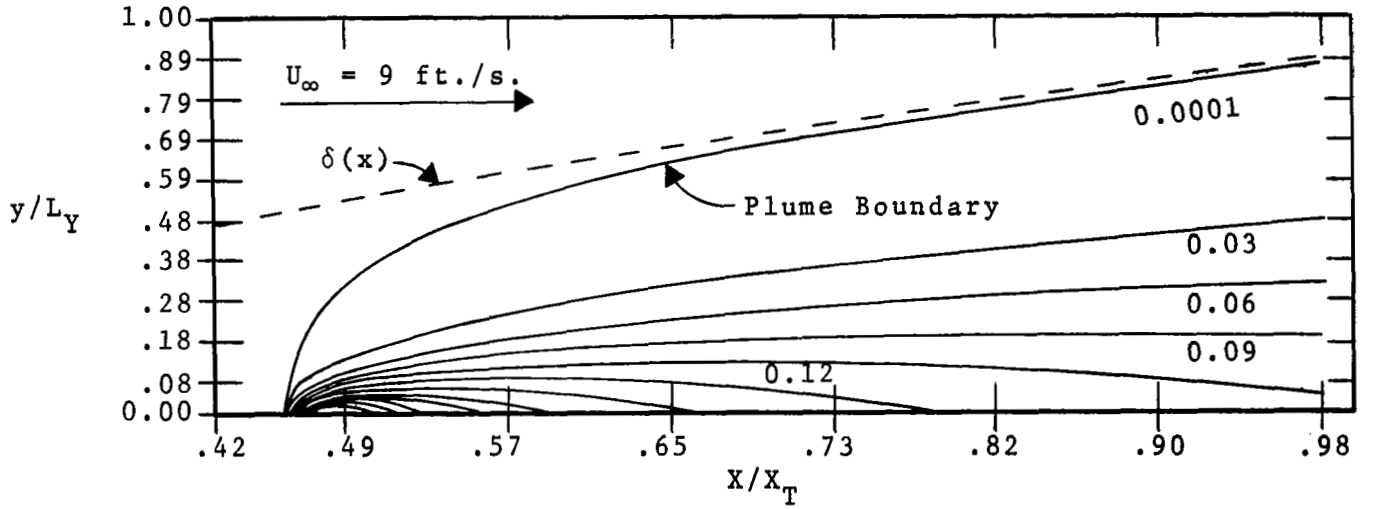

Figure 15. Lines of Constant Concentration Predicted for a Source Located on the Surface

Source Location: X/X_T = 0.4786 , y/L_Y = 0.2857

Field Length = 39.93 ft. XSTART = 30.08 ft.

Field Height = 1.38 ft. NSIY = 45

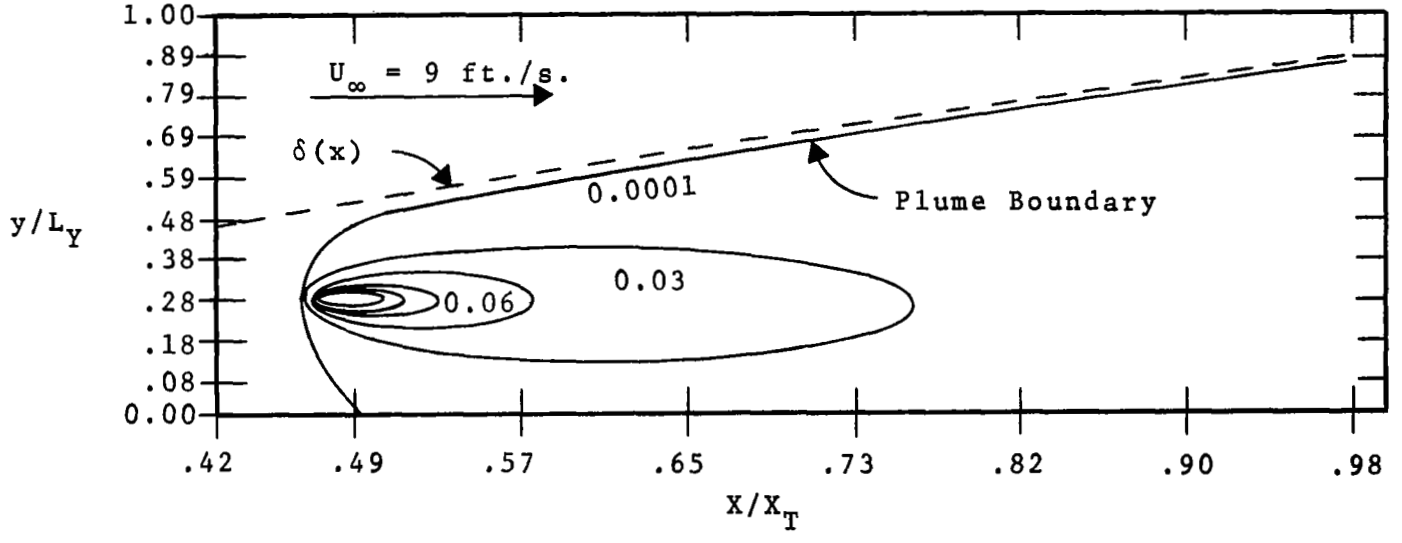

Figure 16. Lines of Constant Concentration Predicted for a Source Located Above the Surface

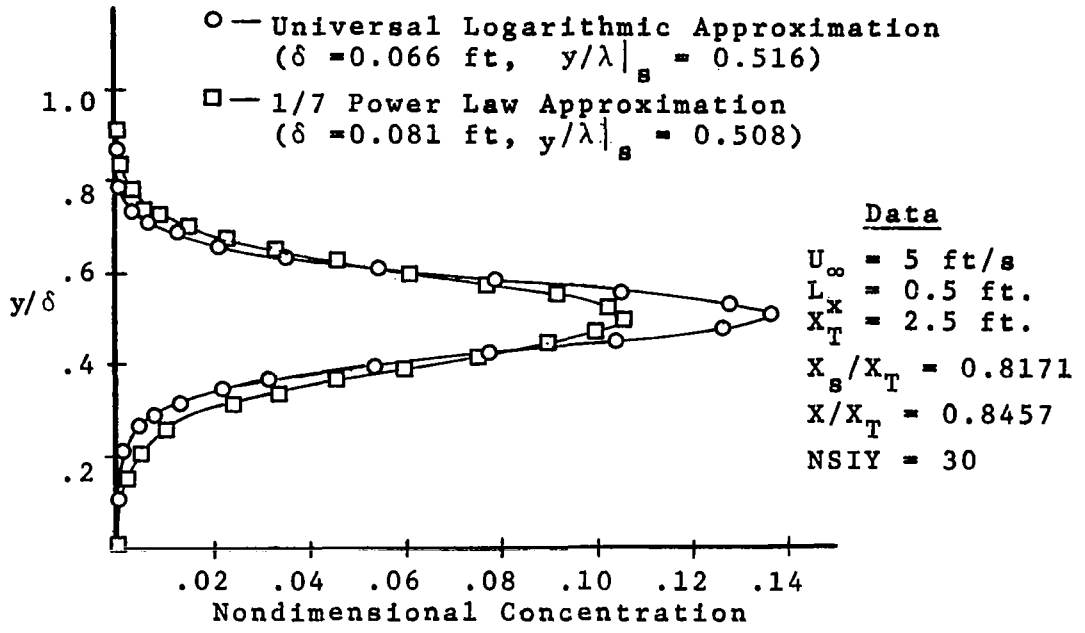

(a)

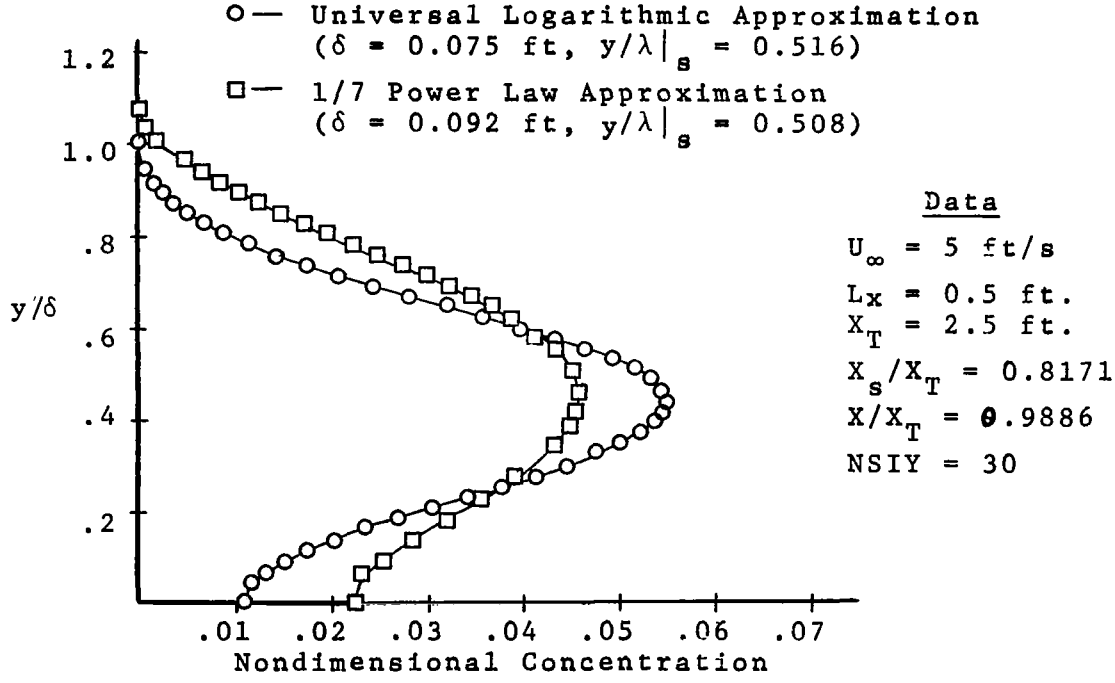

(b)

Figure 17. Comparison of Logarithmic and One-Seventh Power Law Concentration Profile Approximations

TABLE I: EFFECTS OF AN ARTIFICIALLY INDUCED VERTICAL VELOCITY COMPONENT ON THE RATE OF PLUME GROWTH

		V_s = 0.0 ft./s.		V_s = 0.015 ft./s.	
x ~ cm.	$d\delta/dx$	$d\lambda/dx$	β	$d\lambda/dx$	β
34.77	.1628-01	.3579-01	.5749-01	.3669-01	.5758-01
104.3	.1607-01	.1760-01	.1636+00	.1840-01	.1615+00
173.8	.1588-01	.1527-01	.2273+00	.1608-01	.2235+00
243.4	.1570-01	.1344-01	.2918+00	.1429-01	.2840+00
312.9	.1553-01	.1240-01	.3437+00	.1289-01	.3431+00
382.4	.1538-01	.1144-01	.3943+00	.1226-01	.3834+00
452.0	.1523-01	.1048-01	.4500+00	.1132-01	.4343+00
521.5	.1509-01	.1011-01	.4822+00	.1065-01	.4782+00
591.0	.1496-01	.9340-02	.5394+00	.1022-01	.5121+00
660.6	.1483-01	.9129-02	.5586+00	.9649-02	.5541+00
730.1	.1471-01	.8550-02	.6054+00	.9385-02	.5792+00
799.6	.1460-01	.8371-02	.6256+00	.8939-02	.6162+00
869.2	.1449-01	.7975-02	.6627+00	.8738-02	.6368+00
938.7	.1438-01	.7781-02	.6836+00	.8434-02	.6653+00
1008.0	.1428-01	.7589-02	.7048+00	.8298-02	.6805+00

U_∞ = 9.0 ft./s.

L_x = 39.92 ft.

L_y = 25.09 in.

δ_{max} = 14.85 in.

Dist. from L.E. of Plate to L.E. of Field = 30.08 ft.

Reynolds Number at Leading Edge of Field = .1728+07

Reynolds Number at Trailing Edge of Field = .4020+07

Number of Δy-steps Inside B.L. at δ_{max} = 30

TABLE II: EFFECTS OF AN ARTIFICIALLY INDUCED VERTICAL VELOCITY COMPONENT ON THE RATIO OF PLUME THICKNESS TO BOUNDARY LAYER THICKNESS

	V_s = 0.00 ft./s.	V_s = 0.015 ft./s.
x ~ cm.	λ/δ	λ/δ
34.77	.1264	.1298
104.3	.1792	.1849
173.8	.2186	.2262
243.4	.2498	.2584
312.9	.2743	.2847
382.4	.2935	.3058
452.0	.3098	.3228
521.5	.3231	.3377
591.0	.3343	.3499
660.6	.3438	.3605
730.1	.3519	.3695
799.6	.3588	.3774
869.2	.3648	.3841
938.7	.3698	.3902
1008.0	.3745	.3954

U_∞ = 9.0 ft./s.

L_x = 39.92 ft.

L_y = 25.09 in.

δ_{max} = 14.85 in.

Distance from Leading Edge of Plat to Leading Edge of field = 30.08 ft.

Number of steps inside boundary layer at δ_{max} = 30

APPENDIX A: DETERMINATION OF THE LOCAL VELOCITY COMPONENTS

First consider the universal logarithmic velocity profile. For Reynolds numbers less than 10^6 we may use the following forms to represent the velocity profile in the turbulent boundary layer. For $\eta \leq 5$, where $\eta = \frac{yu_*}{\nu}$, a linear profile is satisfactory. That is

$$\frac{u}{u_*} = \eta \quad , \text{ where } u_* = \text{shear velocity.} \tag{A-1}$$

For values of η between 5 and $\eta_\delta = \frac{\delta u_*}{\nu}$ we have

$$\frac{u}{u_*} = A \ln \eta + B \quad . \tag{A-2}$$

In this investigation A = 5.85, and B = 5.56. For the above values of the constants A and B, equation (A-2) becomes

$$\frac{u}{u_*} = A \log_{10} \frac{y u_*}{\nu} + B \quad . \tag{A-3}$$

For $y = \delta$, we have

$$\frac{U_\infty}{u_*} = A \log_{10} \frac{\delta u_*}{\nu} + B \quad . \tag{A-4}$$

Now

$$c_f' = \frac{\tau_w}{\frac{1}{2} \rho U_\infty^2} \quad . \tag{A-5}$$

Here c'_f is the local value of the skin friction coefficient and τ_w is the shear at the surface. Using the definition of the shear velocity, $u_* = \sqrt{\frac{\tau_w}{\rho}}$ and equation (A-5), we obtain

$$\left(\frac{U_\infty}{u_*}\right)^2 = \frac{2}{c_f'} \quad .$$

Writing equation (A-3) in the usual non-dimensional form

$$\frac{u}{U_\infty} = \frac{u_*}{U_\infty}\left[A \log_{10} \frac{y u_*}{\nu} + B\right]$$

or

$$\frac{u}{U_\infty} = \sqrt{\frac{2}{c_f'}}\left[A \log_{10} \frac{y u_*}{\nu} + B\right]. \qquad \text{(A-6)}$$

From reference [8]

$$c_f' = \left[2 \log_{10} R_x - 0.65\right]^{-2.3}, \qquad \text{(A-7)}$$

and we have

$$u_* = \frac{U_\infty}{\sqrt{2}}\left[\left(2 \log_{10} R_x - 0.65\right)^{-2.3}\right]^{1/2} \qquad \text{(A-8)}$$

where $R_x = U_\infty x/\nu$ with x = distance from the leading edge of the plate. For a given value of x and y we may determine the value of (u/U_∞) using equations (A-6), (A-7), and (A-8). Now a value of δ, the boundary layer thickness, must be determined for a given value of x. If $y = \delta$, from equation (A-6) we have

$$1 = \sqrt{\frac{c_f'}{2}}\left[A \log_{10} \frac{\delta u_*}{\nu} + B\right], \qquad \text{and}$$

$$\frac{\delta u_*}{\nu} = 10^{\left[1/A\left(\sqrt{2/c_f'} - B\right)\right]}. \qquad \text{(A-9)}$$

Hence, a value of $\delta = \delta(x)$ is available.

As a second approximation to the velocity profile in a turbulent boundary layer, the power law form was investigated. Here

$$\frac{u}{U_\infty} = a\left[\frac{y}{\delta}\right]^b \qquad \text{(A-10)}$$

where, for this investigation, a = 1.0 and b = 1/7.

From reference [8]

$$\delta(x) = .37\,x\left[\frac{U_\infty x}{\nu}\right]^{-1/5}, \qquad \text{(A-11)}$$

and

$$u_*^2 = U_\infty^2\ 0.0225\left[\frac{\nu}{U_\infty \delta}\right]^{1/4}. \qquad \text{(A-12)}$$

The vertical components of velocity were obtained from the continuity equation

$$\frac{\partial u}{\partial x} + \frac{\partial v}{\partial y} = 0.$$

Integration of the above, using the trapezoidal rule, yields

$$v_{m,N} = v_{m,N-1} - \frac{\Delta y}{2}\left[\frac{\partial u}{\partial x}_{m,N} + \frac{\partial u}{\partial x}_{m,N-1}\right] - \qquad \text{(A-13)}$$

$$-\frac{\Delta y^3}{12}\left[u(x,\eta)\right]_{x,y,y}.$$

In finite difference form suitable for manipulation in the computer solution, equation (A-13) is written as

$$v_{m,N} = v_{m,N-1} - \frac{\Delta y}{4\Delta x}\left[u_{m+1,N} + u_{m+1,N-1} - u_{m-1,N} - u_{m-1,N-1}\right].$$

Use of the trapezoidal rule produced the best results when compared to other methods of numerical integration for this investigation.

APPENDIX B: ANALYSIS OF THE BOUNDARY CONDITIONS

Except for the point of injection for a surface source, there is no flux of mass either into or out of the surface of the flat plate which bounds the field of study on one side. For the particular case of interest, no mass is allowed to accumulate on or to be absorbed by the surface of the plate. Hence, the boundary condition at the surface is

$$\Psi \frac{\partial c}{\partial y} - v c = 0 \qquad \text{(B-1)}$$

where $v = \underline{v} + V_s$ and $\underline{v}$ = the local vertical component of velocity in the flow field while Vs = the mean fall velocity of the contaminant. At the surface $\underline{v} = 0$ and we have

$$\Psi \frac{\partial c}{\partial y} - V_s c = 0. \qquad \text{(B-2)}$$

Equation (B-1) states that the net rate of supply of contaminant to the region immediately above the surface due to the turbulent mass transfer must be equally and oppositely balanced by the rate of removal due to convection.

Consider the general case of steady flow of a pollutant (j) across a surface, and make the following definitions:

$\dot{m}''$ ≡ the total rate of mass transfer across the boundary,

$\dot{m}_j''$ ≡ $\dot{m}'' m_j$ ≡ the convected flux of component j at the surface

$m_j \equiv$ the mass concentration of pollutant j, and

$\gamma_j \equiv \rho\chi$ which is analogous to μ, the dynamic viscosity.

For no mass flux across the boundary, $\dot{m}'' = 0$.

Using the following illustration we may write a general expression for the mass flux across the boundary.

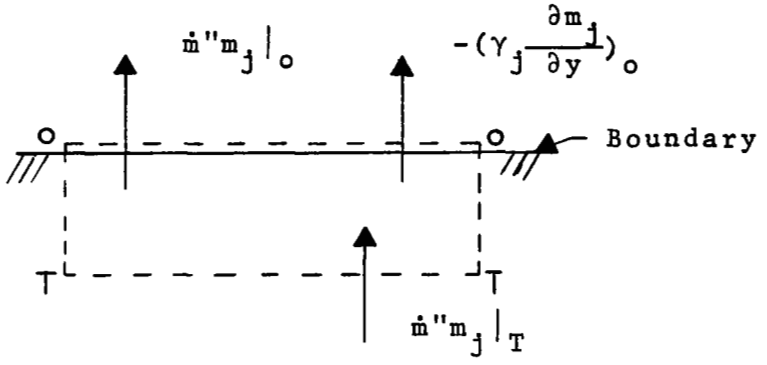

Now $$\dot{m}''m_j|_o - \gamma_j \frac{\partial m_j}{\partial y}|_o - \dot{m}''m_j|_T = 0 \quad . \qquad \text{(B-3)}$$

Since $\dot{m}'' = 0$ we have $$-\gamma_j \frac{\partial m_j}{\partial y}\Big|_o = 0 .$$

Now $\gamma_j \neq 0$. Hence $\frac{\partial m_j}{\partial y}\Big|_o \equiv 0$, and our boundary condition (B-2) becomes

$$\frac{\partial c}{\partial y} = 0 \qquad \text{(B-4)}$$

as $\psi \neq 0$, $V_s|_o = 0$, and $c|_o \neq 0$.

Writing equation (B-4) in finite difference form we have

$$c'_{i+1,1} = \frac{4}{3} c'_{i+1,2} - \frac{1}{3} c'_{i+1,3} \quad , \qquad \text{(B-5)}$$

where the primed notation indicates a nondimensional term.

Far from the source, $y = +\infty$, we require that no concentration gradient can exist between two adjacent points.

Thus $$\frac{\partial c}{\partial y} = 0 \qquad \text{(B-6)}$$

represents the boundary condition at $y = +\infty$. In finite difference form we have $C'_{i+1,J} = C'_{i+1,J-1}$.

The other condition needed is the concentration distribution at some beginning value of x. This condition is referred to as the source condition. For a continuous source this source condition is maintained throughout the solution.

APPENDIX C: DETERMINATION OF THE NONDIMENSIONAL EXCHANGE COEFFICIENTS

To obtain a value of the nondimensional exchange coefficient which will be valid for the two primary regions of interest, the turbulent core of the boundary layer and the external free stream, use was made of the eddy diffusivity concept and the analogy between the methods of transport for mass and momentum. Writing the boundary layer equation for momentum transfer we have

$$\frac{\partial \bar{u}_i}{\partial t} + \bar{u}_j \frac{\partial \bar{u}_i}{\partial x_j} = \frac{\partial}{\partial x_j}\left[\nu \frac{\partial \bar{u}_i}{\partial x_j} - \overline{u_i' u_j'} \right]$$

or

$$\frac{\partial \bar{u}_i}{\partial t} + \bar{u}_j \frac{\partial \bar{u}_i}{\partial x_j} = \frac{\partial}{\partial x_j}\left[\xi \frac{\partial \bar{u}_i}{\partial x_j} \right] \qquad \text{(C-1)}$$

where $\xi = \nu + \epsilon_m$.

Considering mass transport we write

$$\frac{\partial \bar{c}_i}{\partial t} + \bar{u}_j \frac{\partial \bar{c}_i}{\partial x_j} = \frac{\partial}{\partial x_j}\left[\chi \frac{\partial \bar{c}_i}{\partial x_j} - \overline{c_i' u_j'} \right]$$

or

$$\frac{\partial \bar{c}_i}{\partial t} + \bar{u}_j \frac{\partial \bar{c}_i}{\partial x_j} = \frac{\partial}{\partial x_j}\left[\chi_1 \frac{\partial \bar{c}_i}{\partial x_j} \right] \qquad \text{(C-2)}$$

where $\chi_1 = \chi + \epsilon_y$. In the preceding analysis, the bar over the variables indicates an averaged value. Also, ν = kinematic viscosity of the fluid, and χ = the molecular diffusivity coefficient of the contaminant. From equations (C-1) and (C-2) we assume that the mechanics of mass

transport are similar to the mechanics of momentum transport, and hence $\epsilon_y = k(y)\epsilon_m$ where k(y) is some arbitrary function. Therefore we may write $\chi_1 = \chi + k(y)\epsilon_m$. Now, for the two-dimensional flow considered here the shear stress distribution can be represented as

$$\tau_{xy} = \tau_w \left[1 - \frac{y}{\delta} \right] \qquad \text{(C-3)}$$

From a known shear stress and velocity distribution in a two-dimensional flow, the momentum transfer coefficient, ϵ_m, can be computed according to the Boussinesq definition

$$\rho \epsilon_m \frac{\partial u}{\partial y} = \tau_{xy} \quad . \qquad \text{(C-4)}$$

Also, the nondimensional transfer coefficient is defined as

$$\psi = \chi_1 / \bar{\xi} \qquad \text{where} \qquad \bar{\xi} = 1/L_y \int_0^{L_y} \xi \, dy \qquad = \text{the}$$

depth averaged value of the momentum transfer coefficient. We must determine values for ϵ_m, $\bar{\xi}$, and ψ for both approximations to the velocity field over the flat plate. Considering the logarithmic profile first we have

$$\frac{u}{u_*} = A \log_{10} \eta + B \, . \qquad \text{(C-5)}$$

Considering equations (C-3), (C-4), and (C-5) simultaneously, we have

$$\epsilon_m = \frac{\eta \nu}{A} \left[1 - \frac{\eta}{\eta_\delta} \right] ,$$

with

$$\xi = \nu \left[1 + \frac{\eta}{A} \left(1 - \frac{\eta}{\eta_\delta} \right) \right] \qquad \text{(C-6)}$$

for $0 \leq \eta \leq \eta_\delta$,

and $\xi = \nu$ (C-7)

for $\eta > \eta_\delta$.

Averaging the value of ξ over the depth of the field considered (L_y) we obtain

$$\bar{\xi} = \nu \left[\frac{\eta_\delta^2}{6 A \eta_y} + 1 \right] \tag{C-8}$$

where $\eta_\delta = \frac{\delta u_*}{\nu}$ and $\eta_y = \frac{L_y u_*}{\nu}$. Equation (C-8) may also be written as $\bar{\xi} = \frac{u_* \delta^2}{6 A L_y} + \nu$.

Substitution of equation (C-8) into the definition of ψ yields $\psi = \frac{\chi}{\bar{\xi}} = \frac{\chi + k(y)\, \epsilon_m}{\bar{\xi}}$, and

for $0 \leq \eta \leq \eta_\delta$,

$$\psi = \left[\chi + k(\eta) \frac{\eta \nu}{A} - k(\eta) \frac{\eta^2 \nu}{A \eta_\delta} \right] \Big/ \bar{\xi} \tag{C-9}$$

or

$$\psi = \left[\chi + k(y) \left[\frac{y u_*}{A} \left(1 - \frac{y}{\delta} \right) \right] \right] \Big/ \bar{\xi} \quad .$$

As a particular case we assume that k(y) = 1.

For $\eta > \eta_\delta$, $\psi = \frac{\chi}{\bar{\xi}}$. (C-10)

In addition to the value of ψ for various positions through the boundary layer, the solution also requires an expression for $\frac{\partial \psi}{\partial y}$. For $0 \leq y \leq \delta$,

$$\frac{\partial \psi}{\partial y} = \frac{u_*}{A \bar{\xi}} \left[1 - 2 \frac{y}{\delta} \right] , \tag{C-11}$$

and for $y > \delta$, $\frac{\partial \psi}{\partial y} = 0$. (C-12)

Now consider power law approximation to the velocity field and its corresponding form of the nondimensional transfer coefficient. For this case

$$\frac{u}{U_\infty} = a\left[\frac{y}{\delta}\right]^b . \tag{C-13}$$

From the simultaneous consideration of equations (C-3), (C-4), and (C-13) we obtain

$$\epsilon_m = \frac{u_*^2\,\delta}{a\,b\,U_\infty}\left[\frac{y}{\delta}\right]^{(1-b)}\left[1 - \frac{y}{\delta}\right] . \tag{C-14}$$

From (C-14) for $0 \le y \le \delta$ we have

$$\xi = \nu\left[1 + \frac{u_*}{a\,b\,U_\infty}\,\frac{u_*\delta}{\nu}\left[\frac{y}{\delta}\right]^{(1-b)}\left[1 - \frac{y}{\delta}\right]\right] , \tag{C-15}$$

or for $0 \le \eta \le \eta_\delta$

$$\xi = \nu\left[1 + \frac{u_*}{a\,b\,U_\infty}\,\eta_\delta\left[\frac{\eta}{\eta_\delta}\right]^{(1-b)}\left[1 - \frac{\eta}{\eta_\delta}\right]\right] .$$

For $y > \delta$, $\xi = \nu$. (C-16)

Averaging ξ over the entire depth of the field we obtain

$$\bar{\xi} = \nu\left[1 + \frac{u_*}{a\,b\,U_\infty}\,\frac{\delta}{L_y}\,\frac{u_*\delta}{\nu}\,\frac{1}{Q}\right] \tag{C-17}$$

where $Q = 6 - 5b + b^2$. Equation (C-17) may also be written as $\bar{\xi} = \nu\left[1 + \frac{u_*}{a\,b\,U_\infty}\,\frac{\eta_\delta^2}{\eta_y}\,\frac{1}{Q}\right]$.

From the definition of the nondimensional transfer coefficient and equation (C-17) we obtain, with $k(y) = 1$,

$$\psi = \left[\chi + \frac{u_*^2 \delta}{a b U_\infty} \left[\frac{y}{\delta}\right]^{(1-b)} \left[1 - \frac{y}{\delta}\right]\right] \Big/ \bar{\xi} \qquad \text{(C-18)}$$

for $0 \leq y \leq \delta$, and for $y > \delta$

$$\psi = \frac{\chi}{\bar{\xi}} \; . \qquad \text{(C-19)}$$

Written in terms of η, equation (C-18) becomes

$$\psi = \left[\chi + \frac{u_* \sqrt{\eta_\delta}}{a b U_\infty} \left[\frac{\eta}{\eta_\delta}\right]^{(1-b)} \left[1 - \frac{\eta}{\eta_\delta}\right]\right] \Big/ \bar{\xi} \; .$$

for $0 \leq \eta \leq \eta_\delta$. Again considering the special case, $k(y) = 1$, we obtain the variation of ψ in the y-direction.

For $0 \leq y \leq \delta$

$$\frac{\partial \psi}{\partial y} = \frac{u_*^2}{a b U_\infty \bar{\xi}} \left[\frac{y}{\delta}\right]^{-b} \left[(1-b) - (2-b)\frac{y}{\delta}\right], \qquad \text{(C-20)}$$

or

$$\frac{\partial \psi}{\partial y} = \frac{u_*^2}{a b U_\infty \bar{\xi}} \left[\frac{\eta}{\eta_\delta}\right]^{-b} \left[(1-b) - (2-b)\frac{\eta}{\eta_\delta}\right].$$

For $y > \delta$

$$\frac{\partial \psi}{\partial y} = 0 \; . \qquad \text{(C-21)}$$

A plot of ψ vs y/δ is given in Figure 14 for the velocity field approximated by the power law profile.

APPENDIX D: STABILITY ANALYSIS OF THE NUMERICAL SOLUTION

Equation (17) may be written as

$$c^{m}_{i+1,j-1} A + c^{m}_{i+1,j} B + c^{m}_{i+1,j+1} C = c^{m-1}_{i+1,j} D + c^{m}_{i,j} E \qquad \text{(D-1)}$$

where $A = -\frac{v}{2\Delta y} + \frac{\partial\psi/\partial y}{2\Delta y} - \frac{\psi}{\Delta y^2}$

$B = \frac{1}{\Delta t} + \frac{u}{\Delta x} + \frac{2\psi}{\Delta y^2}$

$C = \frac{v}{2\Delta y} - \frac{\partial\psi/\partial y}{2\Delta y} - \frac{\psi}{\Delta y^2}$

$D = \frac{1}{\Delta t}$

$E = \frac{u}{\Delta x}$.

Now let

$$\begin{aligned} c^{m}_{i+1,j-1} &= X_{i+1}\ Y_{j-1}\ T_m , \\ c^{m}_{i+1,j} &= X_{i+1}\ Y_j\ T_m , \\ c^{m}_{i+1,j+1} &= X_{i+1}\ Y_{j+1}\ T_m , \\ c^{m-1}_{i+1,j} &= X_{i+1}\ Y_j\ T_{m-1}, \end{aligned} \qquad \text{(D-2)}$$

and

$$c^{m}_{i,j} = X_i\ Y_j\ T_m .$$

Substitution of (D-2) into (D-1) yields

$$X_{i+1}\left[K - \frac{T_{m-1}}{T_m} D\right] - X_i E = 0 \qquad \text{(D-3)}$$

where $$K = \frac{Y_{j-1}}{Y_j} A + B + \frac{Y_{j+1}}{Y_j} C \quad . \tag{D-4}$$

Equation (D-4) may be rewritten as

$$Y_{j-1} A + Y_j [B - K] + Y_{j+1} C = 0 \quad . \tag{D-5}$$

Define a matrix $\underline{L}$ such that $(\underline{L})_{i,j} = \delta_{i-1,j}$.

Then $(\underline{L}\,\underline{Y})_j = \sum_k (\underline{L})_{jk} (\underline{Y})_k = \sum_k \delta_{j-1,k}\, \underline{Y}_k = \underline{Y}_{j-1}$.

Similarly, $(\underline{L}^T)_{i,j} = \delta_{i+1,j}$ so that

$(\underline{L}^T \underline{Y})_j = \underline{Y}_{j+1}$. Substitution of the preceding relations for $\underline{Y}_{j+1}$ and $\underline{Y}_{j-1}$ into equation (D-5) yields

$$\underline{Y} \left[\underline{L} A + \underline{I} (B - K) + \underline{L}^T C \right] = 0 , \tag{D-6}$$

where the matrix $\underline{L}$ is lower triangular, $\underline{L}^T$ is upper triangular, and $\underline{I}$ represents the unity matrix. For a unique solution to exist, the matrix in brackets in equation (D-6) must be singular. Thus $\det \left| \underline{L} A + \underline{I} (B - K) + \underline{L}^T C \right| = 0$. From theorem 4.2 of Varga [12],

$$\det \left| A \underline{L} + (B - K) \underline{I} + C \underline{L}^T \right| = \det \left| (AC)^{1/2} (\underline{L} + \underline{L}^T) + (B - K) \underline{L}^T \right| .$$

Therefore (K-B) is an eigenvalue of the matrix $\sqrt{AC}\,(\underline{L} + \underline{L}^T)$. From Chapter 9 of Issacson [13], the eigenvalues of $(\underline{L} + \underline{L}^T)$ are $2 \cos \frac{\pi P}{J}$, $P = 1, 2, \cdots J-1$.

Therefore $$K = B + 2\sqrt{AC} \cos \frac{\pi P}{J} , \tag{D-7}$$

[14]. Now consider the x and time equation (D-3). Assume

a solution of the form $T_m = \lambda^m$ and $X_i = \lambda^i$.

Substitution of these assumed solution forms into (D-3) yields

$$\lambda = \frac{D+E}{K} . \qquad \text{(D-8)}$$

For stability, $|\lambda| < 1$ is required. Therefore the stipulation that $-1 < \frac{D+E}{K} < +1$ was investigated for both positive and negative values of K with the following results.

(a) No stability conditions exist in the y-direction since the equations are actually solved along the y-coordinate by a direct method.

(b) If Δy is such that K is real and negative, where

$$K = \frac{1}{\Delta t} + \frac{u}{\Delta x} + \frac{2\psi}{\Delta y^2} + 2\left[\frac{\psi^2}{\Delta y^4} - \frac{(v - \partial\psi/\partial y)^2}{4\Delta y^2}\right]^{1/2} \cos\frac{\pi P}{J}$$

and $\Delta y^2 \leq \frac{4\psi^2}{(v - \partial\psi/\partial y)^2}$, then the conditions

$\Delta t < -4\psi u \Big/ \left[(v - \partial\psi/\partial y)^2 \Delta x + 4\psi u\right]$ and $\psi < 0$ must be satisfied. This condition is physically unrealistic since $\psi \sim \epsilon_y \epsilon_m < 0$ implies a negative coefficient of eddy diffusivity.

(c) Other than the stability condition established in (b) above, the solution is stable for all cases where

(1) K is real and greater than zero with

$$\Delta y^2 \leq \frac{4\psi^2}{(v - \partial\psi/\partial y)^2} \quad \text{and} \quad \Delta t > 0 \quad \text{, and}$$

(2) K is complex and $|K|$ is either positive or negative with

$$\Delta y > \frac{2\psi}{(v - \partial\psi/\partial y)} \quad \text{and} \quad \Delta t > 0 .$$

APPENDIX E: DESCRIPTION AND LISTING OF THE COMPUTER PROGRAM

The description of the computer program is divided into several segments as follows:

a. definition of input variables,

b. discussion of options available,

c. discussion of output,

d. discussion of operations of the different routines, and

e. listing of the computer program.

a. The definitions of the required input variables are as follows:

IOPU = an integer which controls the optional output of the horizontal velocity field.

IOPV = an integer which controls the optional output of the vertical velocity field.

IOPC = an integer which controls the optional output of the initial concentration field.

IOPY = an integer which controls the optional output of the y/δ field matrix.

ICASEA = an integer which controls the execution of the logarithmic velocity profile approximations to the solution of the diffusion equation.

ICASEB = an integer which controls the execution of the power law velocity profile approximations to the solution of the diffusion equation.

IDATA = an integer which controls the optional output of supplementary data regarding the properties of the turbulent transport field.

IPROF = an integer which controls the mode of mass injection, either a two dimensional line profile or line source injection.

ISLOT = an integer which controls the nature of the position of the source, slot in the surface of the plate or a line source above the surface.

VS = mean fall velocity, ft./sec.

RHOP = density of the pollutant, slugs/ft.^{3}.

DIFM = molecular diffusion coefficient, ft.^{2}/sec.

DIA = diameter of the injection probes, probes parallel to the direction of the flow and in a plane parallel to the plate surface, in inches.

CCOL = an integer which designates the column, see Figure 2, in the grid system on which the source is located.

CROW = an integer which designates the row in the grid system of Figure 2 on which the source is located. CROW also indicates the highest point on the profile for the injection of a concentration profile.

NOP = an integer which represents the numbers of injection probes per foot for the line source located above the surface.

LBARX = the field length in feet.

XSTART = the x-station at which the leading edge of the concentration field is located.

VR = the freestream velocity, ft./sec.

EP = ε, the criteria for convergence.

NSIY = the number of steps (Δy) inside the boundary layer at the trailing edge of the concentration field.

N1 = an integer which limits the number of convergence checks in the solution.

N2 = an integer which controls the number of time steps executed before the field is checked to determine whether or not it has reached the approximate steady state solution.

The following data is input only if the source is a line source (slot) on the plate surface.

MDOT = mass flux, mg./cm.^{2}sec.

XS = location of the source with respect to the leading edge of the plate, ft.

CSLOT = the concentration of the pollutant at the injection point, mg./cm.^{3}.

If a concentration profile is being read in, each point concentration along the profile must be input. This input procedure is executed in subroutine CONN. The input variable is Q which is dimensionless (c/C_{max}).

b. The optional output from the computer program is available according to the numerical value of the control variables.

IOPU > 0, no initial u-velocity matrix is output.

IOPV > 0, no initial v-velocity matrix is output.

IOPC > 0, no initial concentration field matrix is output.

IOPY > 0, no y/δ field matrix is output.

ICASEA > 0, deletes the solution for the logarithmic velocity profile approximations.

ICASEB > 0, deletes the solution for the power law velocity profile approximations.

IDATA > 0, deletes the output of supplemental data.

IPROF > 0, implies a line source.

ISLOT > 0, mass is injected above the surface.

Some restrictions on the combinations of the above variables are necessary. Either ICASEA or ICASEB must be equal to zero for every run. When a concentration of pollutant is injected into the stream in a profile instead of a line source, the profile must begin on the surface and extend upward to terminate on row CROW.

c. The output from the program is categorized as optional and standard. The standard output is that which is automatically provided with each run, and this output will be discussed first.

(1) The program designates which velocity profile approximation is being run. Profile A

(Logarithmic) or Profile B (Power Law Formula).

(2) The following items are output to identify the physical properties of the problem of interest:

(a) Freestream Velocity,

(b) Field Length,

(c) Field Height,

(d) Boundary Layer Thickness at Trailing Edge of Field,

(e) Dimensionless Boundary Layer Thickness (Used to determine whether or not the boundary layer is turbulent [8]),

(f) Number of steps in the x and y direction,

(g) Nondimensional Dx and Dy,

(h) The injected mass, slugs/ft.sec.,

(i) The injected concentration, slugs/ft.^{3}.

(j) Minimum concentration for visualization (Applies only to pollutants containing carbon particles such as smoke),

(k) Convergence criteria,

(l) Laminar or molecular diffusion coefficient, ft.^{2}/sec.,

(m) Mean fall velocity, ft./sec.

(n) Distance to the leading edge of the field, ft.,

(o) Reynolds number at the leading edge of the field,

(p) Reynolds number at the trailing edge of the field,

(q) Time Factor (An integer used to alter the magnitude of Δt), and

(r) NSIY.

(3) The matrix of coefficients in the tridiagonal matrix for the solution of the point concentrations is output at the beginning and end of the solution to serve as an indicator regarding the convergence of the solution.

(4) The number of time steps required to reach the steady state is output.

(5) The nondimensional concentration field matrix is output.

(6) A C/C_{max} matrix is output.

Output which is optional and is used only as supplementary information to enhance the usefulness of the standard output is as follows:

(1) nondimensional Δt as a function of x,

(2) the boundary layer thickness in feet as a function of x,

(3) $\overline{\xi}$ as a function of x, ft.^{2}/sec.,

(4) u_* as a function of x, ft./sec.,

(5) X/XT as a function of grid position,

(6) y/Ly as a function of grid position,

(7) initial u-velocity matrix, nondimensionalized as $[u/U_\infty]$,

(8) initial v-velocity matrix, nondimensionalized as $[v/U_\infty)(U_\infty\ x/\nu)^{1/2}]$,

(9) If the mass is injected from a slot, output involving the characteristic plume height (cm.), x(cm.), U_∞ (cm.^{2}/sec.), C_{max}(mg./cm.^{3}), λ(cm.), λ/δ, $C_{max}U_\infty$ (mg./cm.^{2}sec.), x/δ, $d\delta/dx$, $d\lambda/dx$, and β is presented.

(10) A y/δ matrix is optional output, and

(11) for slot injection problems a matrix for y/λ is output.

If the optional control parameter IOPV and IOPY have values 0 and 1 respectively, then a dimensional vertical velocity field with dimensions of ft./sec. will be output automatically.

d. The main program reads in the required data, except for the dimensionless concentration profile when the IPROF option is exercised. This main routine also calculates the various problem identification and physical parameters while it coordinates the activities of the various subroutines.

Subroutine CASEA determines elements of the horizontal velocity field (u/U_∞) for the logarithmic profile approximation. It also provides values of ψ(PSI), Δt(DT), $\bar{\xi}$(EM), u_*(USTAR), and δ(DELTA) for use later in the solution.

Subroutine CASEB determines elements of the horizontal velocity field (u/U_∞) using the power law formula. It also provides the additional boundary layer and transport properties listed above for subroutine CASEA.

Subroutine VCOMP accepts grid point values for the horizontal velocity components from either of subroutine CASEA or CASEB and calculates a dimensional and a nondimensional form of the local vertical velocity components. The calculations of the vertical velocity components are made by integrating the continuity equation numerically.

Subroutine CONN actually solves the diffusion equation utilizing information obtained from the supporting routines. Of particular interest is the fact that an injection of mass into the boundary layer using a profile injection is done so by reading a value of Q(CCOL, K), When K = 1, CROW, into subroutine CONN. Subroutine CONN contains the entire solution of the diffusion equation to include the calculation of $\partial\psi/\partial y|_{i+1,j} = R$ for each particular approximation being executed for a given run. This subroutine does however rely upon subroutine TRIDAG for the actual manipulation of the tridiagonal matrix. The nondimensional concentration at the surface is named CC(M + 1, 1) while the nondimensional concentration at j = J is CC(M + 1, J). The boundary conditions in finite difference form are idenitfied in the subroutine for easy access.

Subroutine TRIDAG manipulates the tridiagonal matrix generated in subroutine CONN. Comments in the subroutine itself describe its activities.

Subroutine PRINT handles the output, both optional and standard, from the various subroutines. Various comment

statements within the subroutine itself identify the segments and functions of the subroutine.

e. A complete listing of the main program with its supporting subroutines follows.

```
C      XSTART = DIST. FROM L.E. OF PLATE TO L.E. OF FIELD
C      LBARY = FIELD HEIGHT IN FT.
C      LBARX = FIELD LENGTH, FT.
C      VR = FREESTREAM VEL., FT./SEC.
C      EP = CONVERGENCE CRITERIA
C      NSIY = NO.OF STEPS INSIDE B.L.
C      N1 = ALLOWABLE NO. OF CHECKS FOR CONVERGENCE
C      N2 = NO.OF TIME STEPS BETWEEN CONVERGENCE CHECKS
C      DY = NON-DIM. STEP SIZE IN Y-DIR.
C      DX = NON-DIM. STEP SIZE IN X-DIR.
C      NOP = NO. OF INJECTION PROBES PER UNIT DEPTH
C      DIA = DIA. OF INJECTION PROBES, IN.
C      DIFM = LAM. MOM. DIFFUSION COEFF., FT.2/SEC.
C      SC = LAMINAR SCHMIDT NO.
C      CCOL = COL.DESIGNATION FOR DISPERSANT INJECTION
C      CROW = ROW DESIGNATION FOR DISPERSANT INJECTION
C      AMVC = ABSOLUTE MIN. CONCENTRATION FOR VISUALIZATION
C      IOPU>0, NO INITIAL U-VEL. MATRIX IS OUTPUT
C      IOPV>0, NO INITIAL V-VEL. MATRIX IS OUTPUT
C      IOPC>0, NO INITIAL CONCENTRATION MATRIX IS OUTPUT
C      IOPY>0, NO Y/DELTA MATRIX IS OUTPUT
C      ICASEA>0, DELETES THE SOL. FOR VEL. FIELD PROFILE A
C      ICASEB>0, DELETES THE SOL. FOR VEL. FIELD PROFILE B
C      IDATA>0, DELETES OUTPUT OF EXTRA DATA, ETC.
C      IPROF>0, INPUT POINT SOURCE CONCENTRATION
C      IPROF=0, INPUT SOURCE CONCENTRATION PROFILE
C      ISLOT=0, MASS IS INJECTED FROM SLOT, MG/CM/SEC
C      XS=X-STATION OF SLOT IN PLATE, FT.
       DOUBLE PRECISION CSLOT,CMX(36),SLM(36)
       DOUBLE PRECISION SLAM(36),CMAX(36),SLOD(36)
       DOUBLE PRECISION DTL,DTN,Y2,Y1,CLAM,DYY
       DOUBLE PRECISION DX,DY,SNU,DT(36),DELTA(36),EM(36),UST
      &AR(36)
       DOUBLE PRECISION U(36,50),V(36,50),CC(36,50),PSI(36,50
      &)
       COMMON U,CC,V,DT,PSI
       REAL LBARX,LBARY,MDOT
       INTEGER CCOL,CROW
       ICON=1
       READ(5,9911) IOPU,IOPV,IOPC,IOPY,ICASEA,ICASEB,IDATA,I
      &PROF,ISLOT
 9911  FORMAT(9I2)
       READ(5,1)VS,RHOP,DIFM,DIA,CCOL,CROW,NOP
       READ(5,1)LBARX,XSTART,VR,EP,NSIY,N1,N2
   1   FORMAT(4F10.0,3I2)
       IF(ISLOT.EQ.0) READ(5,1193) MDOT,XS,CSLOT
 1193  FORMAT(3F10.0)
       I=36
       J=50
       TFACT=3.00
```

```
      RHO=RHOP
      PI=3.1415926535
      SNU=0.0001567
      IFINAL=I - 1
      DX=1.00/(I-1)
      IF(ISLOT.GT.0) XS=(CCOL-1)*DX*LBARX + XSTART
      IF(ICASEA.EQ.0)CALL CASEA(I,J,IDATA,NSIY,DX,XSTART,LBA
     &RX,RHO,     DIFM,SNU,VR,TFACT,DY,LBARY,DELTA,EM,USTAR)
      IF(ICASEB.EQ.0)CALL CASEB(I,J,IDATA,NSIY,DX,XSTART,LBA
     &RX,RHO,     DIFM,SNU,VR,TFACT,DY,LBARY,DELTA,EM,USTAR)
      XT=LBARX + XSTART
      RNLE=VR*XSTART/SNU
      RNTE=VR*XT/SNU
      YYY=.37*XT*((VR*XT/SNU)**(-1./5.))/DSQRT(SNU*XT/VR)
      HTI=LBARY*12.0
      BLMAXF=DY*LBARX*(NSIY-1)
      BLMAXI=BLMAXF*12.0
      IF(ISLOT.EQ.0) GO TO 9853
      NGS=(DIA/DY/LBARX/12.) - 0.50
      KNGS=CROW + NGS - 1
      IF(DIA.LT.(DY*LBARX*12.)) KNGS=CROW
      IF(KNGS.LT.CROW) KNGS=CROW
      MDOT=RHO*VR*PI*NOP*(DIA*DIA/144./4.)
      QQ=MDOT/(VR*DIA/12.)
      QQQ=QQ*32.20
      GO TO 9937
 9853 MDOT=(0.013087125/1000.)*MDOT
      QQ=CSLOT/515.799
      QQQ=QQ*32.2
 9937 AMVC=(0.02/5000.)/QQQ
      WRITE(6,988)VR,LBARX,LBARY,HTI,BLMAXF,BLMAXI,YYY
 988  FORMAT('1FREESTREAM VELOCITY = ',F6.2,' FT/SEC',//,
     &' FIELD LENGTH = ',F5.2,' FT.',//,
     &' FIELD HEIGHT = ',F5.2,' FT. = ',F5.2,' IN.',//,
     &' B.L. THICKNESS AT T.E. OF FIELD = ',E9.4,'FT = ',E9.
     &4,'IN.',//, ' DIMENSIONLESS B.L. THICKNESS = ',F5.2)
      WRITE(6,108) I,J,DX,DY,MDOT,QQ,QQQ,AMVC
 108  FORMAT(//,1H ,'NO. OF STEPS IN X-DIR. = ',I2,10X,
     &'NO. OF STEPS IN Y-DIR. = ',I2,///,
     &' DX = ',E9.4,       10X,'DY = ',E9.4,       ///,
     &' INJECTED MASS = ',E9.4,' SLUG/FT/SEC',///,
     &' INJECTED CONCENTRATION = ',E9.4,' SLUG/FT3 = ',E9.4,
     &' LB/FT3',///,' MIN. CONC. FOR VISUALIZATION = ',
     &F7.4,' NONDIMENSIONALIZED')
      WRITE(6,8877)EP,DIFM,VS,XSTART,RNLE,RNTE,TFACT,NSIY
 8877 FORMAT(///,' CONVERGENCE CRITERIA = ',E9.4,///,
     &' LAMINAR MASS DIFF. COEFF. = ',E9.4,' FT2/SEC',///,
     &' MEAN FALL VELOCITY = ',F7.5,' FT./SEC.',///,
     &' DIST. TO L.E. OF FIELD = ',F5.2,' FT.',///,
     &' REYNOLDS NO. AT L.E. OF FIELD = ',E9.4,///,
```

```
     &' REYNOLDS NO. AT T.E. OF FIELD = ',E9.4,///,
     &' TIME FACTOR = ',F5.2,///,
     &' NO. OF STEPS IN B.L. AT T.E. = ',I2)
      IF(IDATA.GT.0) GO TO 4259
      WRITE(6,4369)
 4369 FORMAT('1',5X,'I',14X,'X/XT',//)
      XT=LBARX + XSTART
      DO 4469 L=1,I
      XOXT=(DX*(L-1)*LBARX + XSTART)/XT
 4469 WRITE(6,4569)L,XOXT
 4569 FORMAT(5X,I2,10X,E9.4)
      WRITE(6,4359)
 4359 FORMAT('1',5X,'J',11X,'Y/LBARY',//)
      DO 4459 L=1,J
      YOLY=DY*(L-1)*LBARX/LBARY
 4459 WRITE(6,4559)L,YOLY
 4559 FORMAT(5X,I2,10X,E9.4)
 4259 IF(IOPY.GT.0) GO TO 6001
      DO 6000 M=1,I
      DO 6000 N=1,J
      IF(XSTART.GT.0) GO TO 7001
      IF(M.GT.1) GO TO 7001
      CC(M,N)=0.00
      GO TO 6000
 7001 Y=DY*DBLE(FLOAT(N-1))*LBARX
      CC(M,N)=Y/DELTA(M)
 6000 CONTINUE
 6001 IF(IOPU.EQ.0) GO TO 6666
      IF(IOPV.EQ.0) GO TO 6666
      IF(IOPY.EQ.0) GO TO 6666
      GO TO 6667
 6666 ICMX=1
      IYLM=1
      CALL PRINT(J,IOPU,IOPV,IOPY,IOPC,ICON,ICMX,IYLM)
 6667 CONTINUE
      CALL CONN(I,J,DX,DY,LBARX,SNU,EM,DELTA,MDOT,VS,N1,N2,
     &XSTART,VR,KNGS,DIA,GQ,EP,CCOL,CROW,ICASEA,ICASEB,NGS,I
     &OPC,USTAR,  DIFM,LBARY,IPROF)
C
C      PROVIDE NECESSARY OUTPUT FOR CORRELATION
C
      WRITE(6,4981)
 4981 FORMAT('1',2X,'J',10X,'X',9X,'R.N.-DELTA',9X,'VR*D',9X
     &,            'CMAX',9X,'LAMBDA',8X,'LAMBDA/DELTA', 5X,'
     &CMAX*VR',                  3X,'X/DELTA',//)
      DO 4434 L=1,I
      CMAX(L)=0.00
      X=((DX*LBARX*(L-1) + XSTART) - XS)*30.48
      RD=VR*DELTA(L)/SNU
      VRSD=VR*DELTA(L)*30.48*30.48
```

```
      DO 4435 K=1,J
      IF(CC(L,K).GT.CMAX(L)) CMAX(L)=CC(L,K)
 4435 CONTINUE
      CMX(L)=CMAX(L)*CSLOT
      CMVR=CMAX(L)*CSLOT*VR*30.48
      IF(ISLOT.GT.0) GO TO 4441
C
C     CAL. CHARACTERISTIC PLUME HEIGHT
C
      CLAM=0.5*CMAX(L)
      IF(CLAM.LE.0.00) GO TO 4441
      DO 4436 K=2,J
      IF(SLAM(L).GT.0.00) GO TO 4436
      XOD=0.00
      Y2=DY*(K-1)*LBARX
      Y1=DY*(K-2)*LBARX
      IF(CC(L,K).GE.CLAM.AND.CLAM.GE.CC(L,K-1)) GO TO 4436
      IF(CC(L,K).LE.CLAM.AND.CLAM.LE.CC(L,K-1)) GO TO 4439
      SLAM(L)=0.00
      SLOD(L)=0.00
      GO TO 4436
 4439 DTL=CC(L,K-1) - CLAM
      DTN=CC(L,K-1) - CC(L,K)
      DYY=Y1 - Y2
      SLAM(L)=Y1 - DYY*DTL/DTN
      SLM(L)=SLAM(L)*30.48
 4440 SLOD(L)=SLAM(L)/DELTA(L)
      XOD=X*SLOD(L)/SLM(L)
 4436 CONTINUE
      GO TO 4356
 4441 SLAM(L)=0.00
      SLOD(L)=0.00
      SLM(L)=0.00
 4356 WRITE(6,4438) L,X,RD,VRSD,CMX(L),SLM(L),SLOD(L),CMVR,X
     &OD
 4438 FORMAT(1X,I2,4X,8(E10.4,5X))
 4434 CONTINUE
      IF(ISLOT.GT.0) GO TO 7781
C
C     SOLVE FOR BETA
C
      WRITE(6,9999)
 9999 FORMAT('1')
       DO 7779 L=1,I
      IF(L.LE.CCOL) GO TO 7777
      IF(L.GE.(I-1)) GO TO 7777
      DDDX=(DELTA(L+1) - DELTA(L-1))/(DX*LBARX*2.)
      DLDX=(SLAM(L+1) - SLAM(L-1))/(DX*LBARX*2.)
      IF(SLOD(L)-0.0) 7777,7777,7778
 7777 BETA=0.00
```

```
      DDDX=0.0
      DLDX=0.00
      GO TO 7779
 7778 BETA=SLOD(L)*DDDX/DLDX
 7779 WRITE(6,7780) DDDX,DLDX,BETA,L
 7780 FORMAT(2X,'DDDX = ',E9.4,5X,'DLDX = ',E9.4,5X,'BETA =
     &',E9.4,     5X,'I = ',I2)
 7781 CONTINUE
C
C     DETERMINE C/CMAX MATRIX
C
      DO 3331 L=1,I
      DO 3331 K=1,J
      IF(CMAX(L) - 0.00) 3332,3332,3333
 3332 CC(L,K)=0.00
      U(L,K)=0.00
      V(L,K)=0.00
      GO TO 3331
 3333 U(L,K)=CC(L,K)/CMAX(L)
      IF(ISLOT.GT.0) GO TO 3331
 3334 V(L,K)=DY*(K-1)*LBARX/SLAM(L)
 3331 CONTINUE
      IOPU=0
      IOPV=0
      IF(ISLOT.GT.0) IOPV=1
      IOPY=1
      IOPC=1
      ICON=1
      ICMX=0
      IYLM=0
      IF(ISLOT.GT.0) IYLM=1
      CALL PRINT(J,IOPU,IOPV,IOPY,IOPC,ICON,ICMX,IYLM)
      STOP
      END
```

```
      SUBROUTINE CASEA(I,J,IDATA,NSIY,DX,XSTART,LBARX,RHO,DI
     &FM,          SNU,VR,TFACT,DY,LBARY,DELTA,EM,USTAR)
C
C     THIS SUBROUTINE CALCULATES THE HORIZ. VEL. FIELD
C     USING THE UNIVERSAL LOGARITHMIC PROFILE.
C
      DOUBLE PRECISION DX,DY,SNU,RN,DELT,USTARM,DELTAM,X,Y,C
     &I
      DOUBLE PRECISION U(36,50),U1(38,50),V(36,50),PSI(36,50
     &)
      DOUBLE PRECISION DELTA(36),EM(36),DT(36),USTAR(36)
      DOUBLE PRECISION CFL(36),DELTN(36),CFLM,CC(36,50)
      COMMON U,CC,V,DT,PSI
      REAL LBARX,LBARY
      WRITE(6,55)
   55 FORMAT(' THE FOLLOWING DATA WAS COMPILED USING VEL. PR
     &OFILE A',//)
      A=5.85
      B=5.56
      DO 1 K=1,I
      X=DX*(K-1)*LBARX + XSTART
      IF(X-0.0)2,3,2
    3 U(1,1)=0.00
      DO 4 L=2,J
    4 U(1,L)=1.00
      DELTA(1)=0.00
      EM(1)=DIFM
      USTAR(1)=0.00
      CFL(1)=0.00
      DELTN(1)=0.00
      DT(1)=DX*DIFM/TFACT/VR/LBARX
      GO TO 1
    2 RN=VR*X/SNU
      USTAR(K)=(VR/SQRT(2.))*SQRT((2.*ALOG10(RN)-0.65)**(-2.
     &3))
      CFL(K)=(2.*ALOG10(RN)-0.65)**(-2.3)
      DELTN(K)=10.**((1./A)*(DSQRT(2./CFL(K))-B))
      DELTA(K)=DELTN(K)*SNU/USTAR(K)
    1 CONTINUE
      DY=DELTA(I)/LBARX/(NSIY-1)
      LBARY=DY*(J-1)*LBARX
C
C     CALCULATE U-VEL. FIELD
C
      DO 11 K=1,I
      EM(K)=(USTAR(K)*DELTA(K)*DELTA(K)/6./A/LBARY) + SNU
      DT(K)=DX*EM(K)/LBARX/VR/TFACT
      DO 11 L=1,J
      Y=DY*(L-1)*LBARX
      YY=Y*USTAR(K)/SNU
```

```
      IF(Y-DELTA(K)) 15,15,16
   15 CONTINUE
      IF(YY - 5.) 5,6,6
    5 U(K,L)=YY*USTAR(K)/VR
      GO TO 23
    6 U(K,L)=(A*ALOG10(YY)+B)*USTAR(K)/VR
   23 CI=DIFM + (Y*USTAR(K)/A)*(1.-Y/DELTA(K))
      GO TO 31
   16 CI=DIFM
      U(K,L)=1.00
   31 PSI(K,L)=CI/EM(K)
   11 V(K,L)=0.00
C
C     CAL.EXTRA ELEMENTS FOR V-VEL. FIELD CAL.
C
      IEXTRA=I + 2
      DO 18 K=1,IEXTRA
      IF(XSTART-0.00) 19,20,19
   20 IF(K.EQ.IEXTRA) GO TO 19
      IF(K.GT.1) GO TO 21
      DO 22 L=1,J
   22 U1(K,L)=1.00
      GO TO 18
   19 IF(K.EQ.IEXTRA) GO TO 30
      IF(K.GT.1) GO TO 21
      IF(K.EQ.1) KL=-1
   30 IF(K.EQ.IEXTRA) KL=I
      XM=XSTART + DX*KL*LBARX
      RN=VR*XM/SNU
      USTARM=(VR/SQRT(2.))*SQRT((2.*ALOG10(RN)-0.65)**(-2.3)
     &)
      CFLM=(2.*ALOG10(RN)-0.65)**(-2.3)
      DELT=10.**((1./A)*(DSQRT(2./CFLM)-B))
      DELTAM=DELT*SNU/USTARM
      DO 24 L=1,J
      Y=DY*(L-1)*LBARX
      YY=Y*USTARM/SNU
      IF(Y-DELTAM) 25,25,26
   25 CONTINUE
      IF(YY-5.) 27,28,28
   27 U1(K,L)=YY*USTARM/VR
      GO TO 24
   28 U1(K,L)=USTARM*(A*ALOG10(YY)+B)/VR
      GO TO 24
   26 U1(K,L)=1.00
   24 CONTINUE
      GO TO 18
   21 DO 29 LL=1,J
   29 U1(K,LL)=U(K-1,LL)
   18 CONTINUE
```

```
C
C     CAL. VERT.-VEL.FIELD
C
      CALL VCOMP(I,J,DX,DY,VR,XSTART,LBARX,DELTA,U1)
      IF(IDATA.GT.0) GO TO 111
      WRITE(6,12)
   12 FORMAT('1',T4,'I',T25,'DT',T45,'DELTA',T67,'EM',T89,'U
     &STAR',      T112,'X',/,T3,'(-)',T25,'(-)',T46,'(FT)',T
     &65,'(FT2/S)',T89,       '(FT/S)',T110,'(FT)',//)
      DO 13 K=1,I
      X=XSTART + DX*(K-1)*LBARX
      WRITE(6,14) K,DT(K),DELTA(K),EM(K),USTAR(K),X
   14 FORMAT(3X,I2,12X,5(E10.4,12X))
   13 CONTINUE
  111 RETURN
      END
```

```
      SUBROUTINE CASEB(I,J,IDATA,NSIY,DX,XSTART,LBARX,RHO,DI
     &FM,          SNU,VR,TFACT,DY,LBARY,DELTA,EM,USTAR)
C
C     THIS SUBROUTINE CALCULATES THE HORIZ. VEL. FIELD
C     USING THE POWER LAW PROFILE.
C
      DOUBLE PRECISION ETAY,ETAD,ETA,SKI,EOED
      DOUBLE PRECISION DX,DY,SNU,DELTAM,X,Y,CC(36,50)
      DOUBLE PRECISION U(36,50),U1(38,50),V(36,50),PSI(36,50
     &)
      DOUBLE PRECISION DELTA(36),EM(36),DT(36),USTAR(36)
      COMMON U,CC,V,DT,PSI
      REAL LBARX,LBARY
      WRITE(6,25)
   25 FORMAT(' THE FOLLOWING DATA WAS COMPILED USING VEL. PR
     &OFILE B',//)
      A=1.00
      B=1./7.
      Q=6. - (5.*B) + (B*B)
      XT=LBARX + XSTART
      DY=.37*XT*((SNU/VR/XT)**(1./5.))/LBARX/(NSIY-1)
      LBARY=DY*LBARX*(J-1)
      DO 1 K=1,I
      X=DX*(K-1)*LBARX + XSTART
      DELTA(K)=.37*X*((SNU/VR/X)**(1./5.))
      IF(X-0.0) 2,3,2
    3 TO=0.00
      GO TO 4
    2 TO=RHO*VR*VR*.0225*((SNU/VR/DELTA(K))**(.25))
    4 USTAR(K)=DSQRT(TO/RHO)
      ETAY=LBARY*USTAR(K)/SNU
      ETAD=DELTA(K)*USTAR(K)/SNU
      EM(K)=SNU*(1.+USTAR(K)*ETAD*ETAD/A/B/VR/ETAY/Q)
      IF(X-0.0) 6,6,5
    6 DT(K)=DX*DIFM/TFACT/VR/LBARX
      GO TO 7
    5 DT(K)=DX*EM(K)/LBARX/VR/TFACT
C
C     CAL. U-VEL. FIELD
C
    7 DO 1 L=1,J
      Y=DY*(L-1)*LBARX
      ETA=Y*USTAR(K)/SNU
      EOED=ETA/ETAD
      IF(Y-DELTA(K)) 15,15,16
   15 U(K,L)=(Y/DELTA(K))**B
      SKI=DIFM+USTAR(K)*SNU*ETAD*(EOED**(1.-B))*(1.-EOED)/A/
     &B/VR
      PSI(K,L)=SKI/EM(K)
      GO TO 1
```

```
   16  U(K,L)=1.00
       PSI(K,L)=DIFM/EM(K)
    1  V(K,L)=0.00
       IEXTRA=I + 2
C
C      CAL. EXTRA ELEMENTS FOR V-VEL. FIELD CAL.
C
       DO 18 K=1,IEXTRA
       IF(XSTART-0.0) 19,20,19
   20  IF(K.EQ.IEXTRA) GO TO 19
       IF(K.GT.1) GO TO 21
       DO 22 L=1,J
   22  U1(K,L)=1.00
       GO TO 18
   19  IF(K.EQ.IEXTRA) GO TO 30
       IF(K.GT.1) GO TO 21
       IF(K.EQ.1) KL=-1
   30  IF(K.EQ.IEXTRA) KL=I
       XM=XSTART + DX*KL*LBARX
       DELTAM=0.37*XM*((SNU/VR/XM)**(1./5.))
       DO 38 L=1,J
       Y=DY*(L-1)*LBARX
       IF(Y.LE.DELTAM) U1(K,L)=A*((Y/DELTAM)**B)
       IF(Y.GT.DELTAM) U1(K,L)=1.00
   38  CONTINUE
       GO TO 18
   21  DO 29 LL=1,J
   29  U1(K,LL)=U(K-1,LL)
   18  CONTINUE
C
C      CAL. VERT-VEL. FIELD
C
       CALL VCOMP(I,J,DX,DY,VR,XSTART,LBARX,DELTA,U1)
       IF(IDATA.GT.0) GO TO 11
       WRITE(6,12)
   12  FORMAT('1',T4,'I',T25,'DT',T45,'DELTA',T67,'EM',T89,'U
      &STAR',      T112,'X',/,T3,'(-)',T25,'(-)',T46,'(FT)',T
      &65,'(FT2/S)',T89,       '(FT/S)',T110,'(FT)',//)
       DO 13 K=1,I
       X=XSTART + DX*(K-1)*LBARX
       WRITE(6,14) K,DT(K),DELTA(K),EM(K),USTAR(K),X
   14  FORMAT(3X,I2,12X,5(E10.4,12X))
   13  CONTINUE
   11  RETURN
       END
```

```
      SUBROUTINE VCOMP(I,J,DX,DY,VR,XSTART,LBARX,DELTA,U1)
      COMMON U,CC,V,DT,PSI
      DOUBLE PRECISION U1(38,50),V(36,50),U(36,50),DT(36),PS
     &I(36,50)
      DOUBLE PRECISION DX,DY,SNU,X,CON,DELTA(36),CC(36,50)
      REAL LBARX
      SNU=0.0001567
      IEXTRA=I + 2
      DO 1 K=1,IEXTRA
      DO 1 L=1,J
    1 U1(K,L)=U1(K,L)*VR
      DO 2 M=1,I
      MM=M + 1
      DO 2 N=2,J
      IF(XSTART.LE.0.) V(1,N)=0.00
      IF(XSTART.LE.0.00.AND.M.EQ.1) GO TO 2
      IF(N-2) 3,3,4
C     TRAPEZOIDAL RULE
    4 CONTINUE
    3 V(M,N)=V(M,N-1)-(DY/DX/4.)*(U1(MM+1,N)+U1(MM+1,N-1)-(U
     &1(MM-1,N)+  U1(MM-1,N-1)))
    2 CC(M,N)=V(M,N)
      DO 400 M=1,I
      X=DX*(M-1)*LBARX + XSTART
      CON=DSQRT(VR*X/SNU)
      DO 400 N=1,J
  400 V(M,N)=(V(M,N)/VR)*CON
      RETURN
      END
```

```
      SUBROUTINE TRIDAG(JF,L,A,B,C,D,V,UJ,UONE)
C
C     SOLUTION OF A SYSTEM OF LINEAR EQUATIONS HAVING A TRID
     &IAGONAL
C     COEFFICIENT MATRIX.
C
C     THE EQUATIONS ARE NUMBERED FROM JF TO L, AND THEIR SUB
     &-DIAGONAL,
C     DIAGONAL AND SUPER-DIAGONAL COEFFICIENTS ARE STORED IN
     & THE VECTORS
C     A, B, AND C.  THE COMPUTED SOLUTION VECTOR V(JF)....V(
     &L) IS STORED
C     IN THE VECTOR V.
C
      DOUBLE PRECISION A(50),B(50),C(50),D(50)
      DOUBLE PRECISION V(50),BETA(50),GAMMA(50),UONE,UJ
C
C     .....COMPUTE INTERMEDIATE VECTORS BETA AND GAMMA.....
C
      BETA(JF)=B(JF)
      GAMMA(JF)=D(JF)/BETA(JF)
      JFP1= JF + 1
      DO 100 I=JFP1,L
      BETA(I)=B(I) - A(I)*C(I-1)/BETA(I-1)
  100 GAMMA(I)=(D(I) - A(I)*GAMMA(I-1))/BETA(I)
C
C     .....COMPUTE FINAL SOLUTION VECTOR V.....
C
      LAST=L - JF
      V(1)=UONE
      V(L)=UJ
      DO 200 K=1,LAST
      I=L - K
  200 V(I)=GAMMA(I) - C(I)*V(I+1)/BETA(I)
      RETURN
      END
```

```
      SUBROUTINE CONN(I,J,DX,DY,LBARX,SNU,EM,DELTA,MDOT,VS,N
     &1,N2,       XSTART,VR,KNGS,DIA,QQ,EP,CCOL,CROW,ICASEA,
     &ICASEB,NGS,IOPC,USTAR,  DIFM,LBARY,IPROF)
      COMMON U,CC,V,DT,PSI
      DOUBLE PRECISION DX,DY,TDX,TDY,DXS,DYS,SNU,R
      DOUBLE PRECISION U(36,50),CC(36,50),U1(38,50),V(36,50)
      DOUBLE PRECISION DT(36),PSI(36,50),EM(36),DELTA(36),US
     &TAR(36)
      DOUBLE PRECISION Q(36,50),A(50),B(50),C(50),D(50),Z(50
     &),CON
      REAL LBARX,MDOT,LBARY
      INTEGER CCOL,CROW
C
C     INITIALIZE CONDITIONS
C
      IOPU=1
      IOPV=1
      IOPY=1
      ICON=1
      ICMX=1
      IYLM=1
      DO 12 K=1,I
      X=DX*(K-1)*LBARX + XSTART
      IF(X-0.) 121,121,123
  123 CON=DSQRT(VR*X/SNU)
      GO TO 122
  121 CON=0.00
  122 DO 12 KK=1,J
      Q(K,KK)=0.00
      U(K,KK)=U(K,KK)*VR*LBARX/EM(K)
      V(K,KK)=(V(K,KK)*VR/CON)*LBARX/EM(K)
      U1(K,KK)=0.00
   12 CC(K,KK)=0.00
      IF(IPROF.EQ.0) GO TO 4259
      DO 1101 KKK=CROW,KNGS
      IF(NGS.EQ.0) NGS=1.00
      Q(CCOL,KKK)=1.00
      V(CCOL,KKK)=V(CCOL,KKK) + VS*LBARX/EM(CCOL)
      U1(CCOL,KKK)=1.00
 1101 CC(CCOL,KKK)=1.00
      GO TO 7252
C
C     READ IN DIMENSIONLESS CONC. PROFILE
C
 4259 DO 5298 K=1,CROW
      READ(5,598) Q(CCOL,K)
  598 FORMAT(F10.0)
      V(CCOL,K)=V(CCOL,K) + VS*LBARX/EM(CCOL)
      CC(CCOL,K)=Q(CCOL,K)
 5298 U1(CCOL,K)=Q(CCOL,K)
```

```
 7252 IFIRST=CCOL - 1
      IF(CROW.GT.1) IFIRST=CCOL
      IF(IOPC.EQ.0) CALL PRINT(J,IOPU,IOPV,IOPY,IOPC,ICON,IC
     &MX,IYLM)
C
C     SOLVE THE CONCENTRATION EQUATION
C
      IFINAL=I - 1
      ICON=0
      DXS=DX * DX
      DYS=DY * DY
      TDX=2. * DX
      TDY=2. * DY
      LL=0
      DO 1420 ITER1=1,N1
      DO 1320 ITER2=1,N2
      DO 1230 M=IFIRST,IFINAL
      IF(IPROF - 0) 4362,4362,4368
 4362 LC=1
      LK=CROW
      GO TO 4369
 4368 LC=CROW
      LK=KNGS
 4369 DO 1301 KKK=LC,LK
      U1(CCOL,KKK)=Q(CCOL,KKK)
 1301 CC(CCOL,KKK)=Q(CCOL,KKK)
      DO 1220 K=1,J
      YOD=DY * (K-1)* LBARX/DELTA(M+1)
      IF(ICASEA.EQ.0) GO TO 1031
      IF(ICASEB.EQ.0) GO TO 1032
 1031 IF(YOD.LE.1.0) R=(USTAR(M+1)/5.85/EM(M+1))*(1.-2.*YOD)
      GO TO 1033
 1032 BB=1./7.
      AA=1.00
      IF(YOD.LE.0.0) R=0.00
      IF(YOD.LE.0.0) GO TO 1033
      IF(YOD.LE.1.0) R=(USTAR(M+1)**2)*(YOD**(-BB))*(1.-BB-(
     &2.-BB)*YOD)  /AA/BB/VR/EM(M+1)
 1033 IF(YOD.GT.1.0)R=0.00
C     THE FOLLOWING F.D. FORMS ARE DERIVED IN APPX.(AT)
      A(K)=R/TDY - (V(M+1,K)/TDY + PSI(M+1,K)/DYS)
      B(K)=1./DT(M+1) + U(M+1,K)/DX + 2.*PSI(M+1,K)/DYS
      C(K)=V(M+1,K)/TDY - (R/TDY + PSI(M+1,K)/DYS)
      D(K)=U1(M+1,K)/DT(M+1) + CC(M,K)*U(M+1,K)/DX
C
C     CONSIDER CONCENTRATIONS AT THE BOUNDARIES
C
      IF(K.EQ.2)GO TO 1034
      IF(K.EQ.(J-1)) GO TO 1035
      GO TO 1220
```

```
 1034 D(K)=D(K) - A(K)*CC(M+1,1)
      GO TO 1220
 1035 D(K)=D(K) - C(K)* CC(M+1,J)
 1220 IF(D(K).LE.(2.E-38)) D(K)=0.00
      IF(M-CCOL) 2110,157,2110
 157  IF(LL-0) 2110,158,2110
 158  LL=1
      WRITE(6,2250)
 2250 FORMAT('1  COEFFICIENT MATRIX',/)
      WRITE(6,2251)
 2251 FORMAT('  Y ',10X,'A',16X,'B',16X,'C',16X,'D',//)
      DO 1225 K=1,J
      Y=DY*(K-1)*LBARX
 1225 WRITE(6,2252) Y,A(K),B(K),C(K),D(K)
 2252 FORMAT(1H ,F4.2,1P4E17.7)
 2110 JROW=2
      UONE=CC(M+1,1)
      UJ=CC(M+1,J)
      CALL TRIDAG(JROW,J,A,B,C,D,Z,UJ,UONE)
      DO 1232 K=1,J
      IF(Z(K).LE.(2.E-38)) Z(K)=0.00
 1232 CC(M+1,K)=Z(K)
C
C     CONSIDER  THE BOUNDARY CONDITIONS
C
      CC(M+1,1)=(4.*CC(M+1,2) - CC(M+1,3))/3.
      CC(M+1,J)=CC(M+1,J-1)
 1230 CONTINUE
      IF(ITER2 - N2) 1318,1320,1320
 1318 DO 1319 M=IFIRST,IFINAL
      DO 1319 K=1,J
      IF(CC(M+1,K).GT.0..AND.U1(M+1,K).LE.0.) V(M+1,K)=V(M+1
     &,K)            + VS*LBARX/EM(M+1)
      IF(CC(M+1,K).LE.0..AND.U1(M+1,K).GT.0.) V(M+1,K)=V(M+1
     &,K)            - VS*LBARX/EM(M+1)
 1319 U1(M+1,K)=CC(M+1,K)
 1320 CONTINUE
C
C     CHECK FOR CONVERGENCE
C
      MI=IFIRST + 1
      MF=IFINAL + 1
      DO 1409 M=MI,MF
      DO 1400 N=1,J
      IF(DABS(CC(M,N)-U1(M,N))-EP) 1400,1400,4001
 1400 U1(M,N)=CC(M,N)
      IF(M-IFINAL) 1409,159,1409
 159  WRITE(6,2250)
      WRITE(6,2251)
      DO 1401 N=1,J
```

```
      Y=DY*(N-1)*LBARX
1401  WRITE(6,2252) Y,A(N),B(N),C(N),D(N)
1409  CONTINUE
      GO TO 5001
4001  MP1=M+1
      DO 1410 L=N,J
1410  U1(M,L)=CC(M,L)
      DO 1420 II=MP1,MF
      DO 1420 L=1,J
1420  U1(II,L)=CC(II,L)
      L=N1 * N2
      WRITE(6,15) MP1,N,L
 15   FORMAT(////,' CONVERGENCE OF C(',I2,',',I2,') DID NOT
     &OCCUR IN ',I5,' TRIES')
5001  CONTINUE
      WRITE(6,120) ITER1,ITER2
120   FORMAT('     ITER1 = ',I2,'     ITER2 = ',I2)
      ICON=0
      CALL PRINT(J,IOPU,IOPV,IOPY,IOPC,ICON,ICMX,IYLM)
      RETURN
      END
```

```
      SUBROUTINE PRINT(J,IOPU,IOPV,IOPY,IOPC,ICON,ICMX,IYLM)
C
C     PRINT VELOCITY MATRICES
C
      COMMON U,CC,V,DT,PSI
      DOUBLE PRECISION U(36,50),V(36,50),CC(36,50),PSI(36,50
     &),DT(36)
      INTEGER OPTN
      IF(ICMX.EQ.0) GO TO 83
      IF(IOPU.GT.0) GO TO 6541
   83 LL=1
      LM=18
      DO 111 NUM=1,2
      IF(ICMX.EQ.0) WRITE(6,425)
  425 FORMAT('1 C/CMAX MATRIX',/)
      IF(ICMX.EQ.0) GO TO 98
      WRITE(6,109)
  109 FORMAT('1 INITIAL U-VELOCITY FIELD',/)
   98 GO TO (30,40),NUM
   30 WRITE(6,110)
  110 FORMAT(' X-STEP  1     2     3     4     5     6     7
     &     8',5X, '9     10    11    12    13    14    15
     & 16    17    18',/,     ' Y-STEP')
      GO TO 42
   40 WRITE(6,115)
  115 FORMAT(' X-STEP 19    20    21    22    23    24    25
     &    26',4X, '27    28    29    30    31    32    33
     & 34    35    36',/,     ' Y-STEP')
   42 DO 1111 K=1,J
      KK=(J-K) + 1
      WRITE(6,112) KK,(U(L,KK),L=LL,LM)
  112 FORMAT(3X,I2,2X,18(F5.3,1X))
 1111 CONTINUE
      LL=LL + 18
  111 LM=LM + 18
 6541 CONTINUE
      IF(IYLM.EQ.0) GO TO 87
      IF(IOPV.GT.0) GO TO 6542
   87 LL=1
      LM=18
      DO 114 NUM=1,2
      IF(IYLM.EQ.0) WRITE(6,426)
  426 FORMAT('1 Y/LAMBDA MATRIX',/)
      IF(IYLM.EQ.0) GO TO 99
      WRITE(6,113)
  113 FORMAT('1 INITIAL V-VELOCITY FIELD',/)
   99 GO TO (31,41),NUM
   31 WRITE(6,110)
      GO TO 43
   41 WRITE(6,115)
```

```
 43   DO 1114 K=1,J
      KK=(J-K) + 1
      WRITE(6,1122) KK,(V(L,KK),L=LL,LM)
1122  FORMAT(3X,I2,2X,18(F5.3,1X))
1114  CONTINUE
      LL=LL+18
114   LM=LM + 18
6542  CONTINUE
      IF(IOPY.EQ.0) OPTN=1
      IF(IOPY.GT.0) OPTN=0
      IF(IOPV.EQ.0.AND.IOPY.GT.0) IOPY=0
      IF(IOPV.EQ.0.AND.ICON.GT.0) IOPY=1
      IF(IOPY.GT.0) GO TO 6543
      LL=1
      LM=18
      DO 444 NUM=1,2
      IF(OPTN.EQ.1) WRITE(6,2225)
2225  FORMAT('1 Y/DELTA MATRIX',//)
      IF(OPTN.EQ.0) WRITE(6,2235)
2235  FORMAT('1 V-VELOCITY FIELD -- DIMENSIONAL',//)
      GO TO (71,81),NUM
 71   WRITE(6,1116)
1116  FORMAT(' X-STEP 1       2       3       4       5       6
     &    7',6X,  '8       9      10      11      12      13
     &14      15      16',5X,    '17      18',/,' Y-STEP')
      GO TO 73
 81   WRITE(6,1117)
1117  FORMAT(' X-STEP 19     20     21      22      23      24
     &  25',5X,    '26      27      28      29      30      31
     & 32      33      34',5X,  '35      36',/,' Y-STEP')
 73   DO 4444 K=1,J
      KK=(J-K) + 1
      WRITE(6,442) KK,(CC(L,KK),L=LL,LM)
442   FORMAT(1X,I2,1X,18(F6.3,1X))
4444  CONTINUE
      LL=LL + 18
444   LM=LM + 18
6543  CONTINUE
      IF(IOPC.GT.0.AND.ICON.GT.0) GO TO 7654
      LL=1
      LM=18
      DO 1333 NUM=1,2
      IF(IOPC.EQ.0) WRITE(6,209)
209   FORMAT('1 INITIAL CONCENTRATION MATRIX',/)
      IF(ICON.EQ.0) WRITE(6,1123)
1123  FORMAT('1 FINAL CONCENTRATION MATRIX',/)
      GO TO (90,91),NUM
90    WRITE(6,1116)
      GO TO 92
91    WRITE(6,1117)
```

```
92    DO 4333 K=1,J
      KK=(J-K) + 1
      WRITE(6,332) KK,(CC(L,KK),L=LL,LM)
332   FORMAT(1X,I2,1X,18(F6.4,1X))
4333  CONTINUE
      LL=LL+ 18
1333  LM=LM + 18
7654  CONTINUE
      RETURN
      END
```

BIBLIOGRAPHY

1. Jobson, Harvey E., and Sayre, William W., "Predicting Concentration Profiles in Open Channels," Journal of the Hydraulics Division, Proceedings of the American Society of Civil Engineers, Vol. 96, No. HY 10, October 1970.

2. Sayre, William W., "Dispersion of Silt Particles in Open Channel Flow," Journal of the Hydraulics Division, Proceedings of the American Society of Civil Engineers, Vol. 95, No. HY 3, May 1969.

3. Morkovin, M. V., "On Eddy Diffusivity Quasi-Similarity and Diffusion Experiments in Turbulent Boundary Layers," International Journal of Heat and Mass Transfer, 8, 1965.

4. Pasquill, F., D. Sc., Atmospheric Diffusion, D. Van Nostrand Company LTD, Windsor House, 46 Victorian Street, London, S.W., 1968.

5. Dyke, Milton Van, Vincenti, Walter G., and Wehausen, J. V., Annual Review of Fluid Mechanics, Vol. 2, Annual Review, Inc., 4139 El Camino Way, Palo Alto, California, 1970.

6. Lumley, John L., and Panofsky, Hans A., "The Structure of Atmospheric Turbulence," Interscience Monographs and Texts in Physics and Astronomy, Volume XII, ed. R. E. Marshak, John Wiley and Sons, New York, 1964.

7. Kays, W. M., Convective Heat and Mass Transfer, McGraw-Hill Book Company, New York, 1966.

8. Schlichting, Herman, Boundary Layer Theory, Sixth Edition, McGraw-Hill Book Company, New York, 1968.

9. Poreh, M., and Cermak, J. E., "Study of Diffusion from a Line Source in a Turbulent Boundary Layer," International Journal of Heat and Mass Transfer, Vol. 7, Permagon Press, Great Britain, 1964.

10. Berlyand, M. Ye, and Onikul, R. I., "Physical Principles of Calculation of Dispersal of Industrial Discharge in the Atmosphere," AICE Survey of USSR Air

Pollution Literature, Volume V, Effects of Meteorological Conditions and Relief on Air Pollution; Air Contaminants - Their Concentration, Transport and Dispersal, ed. Nuttonson, M. Y., American Institute of Crop Ecology, Silver Springs, Maryland, 1970.

11. Lin, C. S., Moulton, R. W., and Putnam, G. L., "Mass Transfer Between Solid Walls and Fluid Streams," Industrial Engineering Chem. 45, 1953.

12. Varga, Richard S., Matrix Iterative Analysis, Prentice Hall, Inc., New Jersey, 1962.

13. Issacson, E. K. and Keller, H. B. Analysis of Numerical Methods, John Wiley and Sons, Inc., New York, 1966.

14. Thompson, J. F., personal interview, November, 1971.

15. Taylor, G. I., "Diffusion by Continuous Movements," 1921, Aerophysics of Air Pollution, ed. Fay, J. A. and Hoult, D. P., American Institute of Aeronautics and Astronautics, Vol. IX, New York, 1969.

16. Sutton, O. G., "A Theory of Eddy Diffusivity in the Atmosphere," 1931, Aerophysics of Air Pollution, ed. Fay, J. A. and Hoult, D. P., American Institute of Aeronautics and Astronautics, Vol. IX, New York, 1969.

17. Monin, A. S. and Obuknov, A. M., "Basic Laws of Turbulent Mixing in the Ground Layer of the Atmosphere," 1954, Aerophysics of Air Pollution, ed. Fay, J. A. and Hoult, D. P., American Institute of Aeronautics and Astronautics, Vol. IX, New York, 1969.

18. Sayre, W. W., "Dispersion of Mass in Open Channel Flow," Hydraulics Paper No. 3, Colorado State University, Fort Collins, Colorado, 1968.

19. Poreh, M., "Diffusion from a Line Source in a Turbulent Boundary Layer," Ph.D. Dissertation, Colorado State University, Fort Collins, Colorado, 1961.